

UNCLASSIFIED

AD NUMBER
AD860696
NEW LIMITATION CHANGE
TO Approved for public release, distribution unlimited
FROM Distribution authorized to U.S. Gov't. agencies and their contractors; Critical Technology; 23 JUN 1969. Other requests shall be referred to Naval Avionics Facility, Indianapolis, IN 46218.
AUTHORITY
usnafi ltr, 10 may 1972

THIS PAGE IS UNCLASSIFIED

AD 860696



TR 1331

23 JUNE 1969

**NAFI publication**  
**APPLIED RESEARCH DEPARTMENT**

**SERVO  
AMPLIFIER /SERVOMOTOR  
COMPATIBILITY  
STUDY**

THIS DOCUMENT IS SUBJECT TO SPECIAL EXPORT CONTROLS  
AND EACH TRANSMITTAL TO FOREIGN GOVERNMENTS OR  
FOREIGN NATIONALS MAY BE MADE ONLY WITH PRIOR APPROVAL  
OF NAVAL AVIONICS FACILITY, INDIANAPOLIS, INDIANA

D D C  
RECEIVED  
OCT 30 1969  
RECEIVED



**NAVAL AVIONICS FACILITY**

**INDIANAPOLIS, INDIANA 46218**

DATE	12 12 1968	<input checked="" type="checkbox"/>
DOC	2475 SECTION	<input checked="" type="checkbox"/>
RECEIVED		<input type="checkbox"/>
POSTMASTER		
BY		
RECEIVED/ATTACHMENT CODES		
EXT.	AVAIL. 12/1/68	SPERM
2		

NAFI TR-1331

NOTICES

The discussions or opinions concerning commercial products herein do not constitute an endorsement or condemnation by the government, nor do they convey or imply the right to a license for use of such products.

PREFACE

The purpose of this study was to establish a criterion which could be used to predict the stability performance of servo amplifier/servomotor combinations. A particular amplifier/motor combination is defined as unstable when there are oscillations in the amplifier output voltage due to the effect of the servomotor impedance on the amplifier internal feedback loop. These oscillations are not to be confused with those of a servo system.

This study develops a technique to obtain the open-loop gain characteristics of servo amplifiers by means of external measurements with no access to the feedback loop and no knowledge of the exact amplifier circuit configuration. With this technique and proper specifications on the servomotor, a worst-case stability dummy load can be specified for testing the stability characteristics of incoming production servo amplifiers. The theory, procedures, and test techniques necessary to obtain the worst-case loads are presented. Amplifier loop gain and load impedance frequency characteristics are examined to determine the frequency range where instability may occur. Specialized computer programs written to aid in the stability determinations are included for future reference. A limited number of servo amplifiers were evaluated, and the results are summarized. Recommendations are made to modify present specifications to include parameters which will insure the stable operation of amplifier/motor combinations.

This work was performed under AIRTASKS A34520/2311/69F17532402 and A34522006/2311/F008-01-15 for Naval Air Systems Command (AIR-52022).

ABSTRACT

This report presents a study of the stability problem (tendency for unwanted oscillation) of a servo amplifier driving a servomotor. Servo amplifier stability is affected by the servomotor impedance being reflected back into the amplifier internal feedback loop.

The servo amplifier/servomotor modeling techniques used for stability evaluation are considered. The study develops techniques for evaluating, testing, and specifying servo amplifier/servomotor combinations with respect to stability. Recommendations are made to modify present specifications to include parameters which will insure stable operation of amplifier/motor combinations. A limited number of commercially available servo amplifiers with standard servomotors are evaluated and results are summarized.

Prepared By: Clifford E. Hogue  
CLIFFORD E. HOGUE

Leonard S. Skwierka  
LEONARD S. SKWIERA

Jack W. Templeton  
JACK W. TEMPLETON

Approved By: Ronald R. Jennings  
RONALD R. JENNINGS, Chief  
Controls Systems Branch

Francis A. Marasco  
FRANCIS A. MARASCO, Manager of  
Experimental Research Division

TABLE OF CONTENTS

	<u>Page</u>
PREFACE -----	ii
ABSTRACT -----	iii
LIST OF FIGURES -----	vi
LIST OF TABLES -----	vii
GLOSSARY OF MOTOR MODEL TERMS -----	viii
I. CONCLUSIONS -----	1
II. RECOMMENDATIONS -----	3
A. DUMMY LOAD USAGE -----	3
B. SERVOMOTOR SPECIFICATION CHANGES -----	4
III. INTRODUCTION -----	7
A. STATEMENT OF PROBLEM -----	7
B. GENERAL DESCRIPTION OF SERVO AMPLIFIER/SERVOMOTOR OPERATION -----	8
IV. SERVO AMPLIFIER/SERVOMOTOR COMPATIBILITY WITH RESPECT TO SPECIFICATIONS AND PRODUCTION TESTING -----	11
V. SERVOMOTOR DISCUSSION -----	15
A. SERVOMOTOR DESCRIPTION -----	15
B. EQUIVALENT SERIES CIRCUIT PARAMETER CORRELATION -----	18
C. COMPLEX EQUIVALENT CIRCUIT PARAMETER DETERMINATION -----	26
VI. SERVO AMPLIFIER DISCUSSION -----	36
A. GENERAL DESCRIPTION -----	36
B. GH OBTAINED BY EXTERNAL MEASUREMENT -----	37
C. HOW TO OBTAIN $Z_{11}$ and $Z_{12}$ (unstable) CURVES FROM GH CURVES -----	38
D. CURVE COMPARISON -----	46
VII. STABILITY DETERMINATION TECHNIQUES -----	48
A. DUMMY LOAD DETERMINATION -----	48
B. TESTING PROCEDURE (AMPLIFIER WITH WORST-CASE DUMMY LOAD) -----	66
C. COMPARISON OF PLOTS $Z$ (unstable) AND $Z_{12}$ FOR WORST-CASE STABILITY DUMMY LOAD -----	66
D. COMPARISON OF THE RESULTS OF THE TWO STABILITY DETERMINA- TION TECHNIQUES -----	68

TABLE OF CONTENTS (Continued)

	<u>Page</u>
VIII. EVALUATION OF SERVO AMPLIFIER PERFORMANCE -----	75
A. CRITERIA FOR EVALUATION OF SERVO AMPLIFIER/SERVO MOTOR COMBINATIONS -----	75
B. SUMMARY OF TEST RESULTS -----	79
C. SUMMARY OF SERVO AMPLIFIER PERFORMANCE -----	79
DISTRIBUTION LIST -----	81

LIST OF FIGURES

<u>Figure</u>		<u>Page</u>
1a.	Servo Amplifier Flow Graph -----	9
1b.	Servo Amplifier Simplified Schematic -----	10
2.	Servo Amplifier Equivalent Circuit -----	13
3.	Equivalent Series Motor Model -----	15
4.	Complex Equivalent Circuit of the Servomotor -----	16
5.	Ideal Dummy Load for the Complex Motor Model -----	17
6.	Plot of $R_s$ Versus $X_{ls}$ for Several Motor Samples -----	19
7.	Plot of $R_{oc}$ Versus $X_{ls}$ for Several Motor Samples -----	27
8.	Matrix of Possible Combinations of Extreme Motor Parameters -----	28
9.	Servomotor Impedance Determination -----	29
10.	Time-Sharing Computer Program for Calculation of Motor Impedances $Z_1$ and $Z_3$ -----	30
11.	Calculated Values of Motor Impedances $Z_1$ and $Z_3$ -----	31
12.	Bode Plots of $Z_1$ and $Z_3$ -----	33
13.	Equivalent Servomotor Circuits -----	34
14.	Flow Diagrams of a Single Loop Amplifier -----	38
15.	Flow Diagrams of a Multiloop Amplifier -----	39
16.	Flow Diagrams of an Amplifier with Internal Loop -----	40
17.	Output Impedance Measurement Circuit -----	41
18.	Flow Chart for Computation of GH and $Z_{unstable}$ -----	42
19.	Card FORTRAN Computer Program for Computation of GH and $Z_{unstable}$ -----	43
20.	Time-Sharing BASIC Computer Program for Computation of GH and $Z_{unstable}$ -----	44
21.	Comparison of $Z_{12}$ and $Z_{unstable}$ Curves to Determine Stability -----	47
22.	Printout of Program to Calculate Load Impedances $Z_{11}$ and $Z_{12}$ (Card FORTRAN Version) -----	51
23.	Printout of Program to Calculate Load Impedances $Z_{11}$ and $Z_{12}$ (Time-Sharing BASIC Version) -----	52
24.	Computer Printout of Performance and Construction Data for the Transformer Design -----	56



LIST OF FIGURES (Continued)

<u>Figure</u>		<u>Page</u>
25a, b.	Comparison of $Z_{12}$ Responses -----	60, 61
26.	Practical Dummy Load for the Complex Equivalent Circuit Motor Model -----	62
27.	Experimental Dummy Load for the Equivalent Circuit Motor Model -----	63
28a.	Practical Equivalent Series Dummy Load -----	64
28b.	Ideal Equivalent Series Dummy Load -----	65
29.	Nyquist Plots -----	68
30.	Stable X-Y Plot -----	76
31.	Low Level Oscillating X-Y Plot -----	77
32.	High Level Oscillating X-Y Plot -----	78

LIST OF TABLES

I.	Coordinates of the Corners of the Parallelograms Defining Regions of Acceptable Motor Parameter Combinations -----	6
II.	Least Squares Best Linear Fit Equations -----	6
III.	Servomotors -----	21
IV.	Servomotor Equivalent Series Circuit Parameters Obtained from Kearfott and NAD, Crane, Indiana -----	23
V.	Servomotor Equivalent Circuit Parameters for Motors Tested at NAFI -----	25
VI.	Definition of Variables Used in Computation of GH and ZL (unstable) -----	45
VII.	Worst-Case Dummy Loads -----	50
VIII.	Definition of Variables Used in the Computation of $Z_{11}$ and $Z_{12}$ -----	53
IX.	Parameter Limits for Worst-Case Power Dummy Loads -----	55
X.	Servo Amplifiers Tested -----	69
XI.	Transfer Function Plot Characteristics -----	71
XII.	Correlation of Stability Tests -----	73
XIII.	Summary of Amplifier Stability -----	80

GLOSSARY OF MOTOR MODEL TERMS

$R_s = R_{AC} + R_{DC}$	-- Series Resistive component of the complex impedance
$R_{AC}$	----- Serie. AC resistance
$R_{DC}$	----- DC resistance of the stator or stator copper loss
$L_s$	----- Series Inductive component of the complex impedance
$X_{Ls}$	----- Series Reactive component of the complex impedance
$L_{Ls}$	----- Stator leakage inductance
$L_{Lr}$	----- Rotor leakage inductance
$L = L_M$	----- Magnetizing inductance
$R_M$	----- Core loss
$R_R$	----- Rotor Resistance
$S$	----- Slip
$R_R/S$	----- Effective rotor resistance
$\frac{L_{LP}}{2}$	----- Leakage inductance in half the primary (stator) which is not magnetically coupled to the other half of the primary winding.

Series Motor Model - A simple model of the servomotor in which the impedance of the control winding is lumped into three series components:

$R_{DC}$ ,  $R_{AC}$ , and  $L_s$ .

Complex Motor Model - A more realistic model of the servomotor in which the inductive coupling between the stator and the rotor of the motor is represented by a symmetric transformer equivalent.

Ideal Equivalent Circuit - An equivalent circuit of the servomotor which was developed theoretically and does not take into consideration parasitics associated with the actual components which will be used to implement the circuit for laboratory testing.

Practical Equivalent Circuits - An extension of the Ideal Equivalent Circuit which includes models for the physical components (and their associated parasitics) used in the experimental dummy loads. These equivalent circuits were established and analyzed using the NAFI CODED circuit analysis program to verify the experimental data measured in the laboratory.

Experimental Equivalent Circuit - An equivalent circuit which schematically represents the configuration of the actual physical components

NAFI TR-1331

utilized in the dummy load for laboratory tests.

EQUIVALENT CIRCUIT

SERIES MODEL

COMPLEX MODEL

Ideal

Fig. 28b Page 65

Fig. 5 Page 17

Practical

Fig. 28a Page 64

Fig. 26 Page 62

Experimental

Fig. 28b Page 65

Fig. 27 Page 63

Similar to Ideal Circuit

# I. CONCLUSIONS

A. Present servo amplifier and servomotor specifications are not sufficient to insure the stable operation of the combination. Many amplifier specifications do not present the range of loads which will result in stable amplifier operation. The effects of the frequency characteristics of the load on the amplifier loop gain are not considered. The servomotor specifications do not usually mention parameters which are important for stability considerations, such as the control winding DC resistance, and the leakage reactance between the halves of the control winding.

B. The standard series equivalent circuit motor model (Fig. 3, page 15) is not sufficient to determine the stability characteristics of a servomotor/servo amplifier combination. This motor model does not simulate the frequency characteristics of the motor except at the operating frequency (400 Hz).

C. The standard series equivalent circuit motor model including the control winding DC resistance ( $R_{oc}$ ), the leakage reactance ( $X_{LL}$ ) and the equivalent transformer between the halves of the control winding (Fig. 28b, page 65) is sufficient to simulate the motor characteristics and to determine the stability performance of the amplifier/motor combinations at frequencies above the operating frequency (400 Hz). For the limited number of amplifiers tested, it was observed that all instabilities occurred at frequencies above 400 Hertz. In general, however, the equivalent series motor model would not be sufficient to test for amplifier/motor combination instabilities because oscillations could occur at frequencies below 400 Hertz.

D. The complex equivalent circuit motor model (Fig. 5 page 17) is sufficient to simulate the frequency characteristics of the servomotors both above and below the operating frequency.

E. Given no external access to servo amplifier feedback loops and no knowledge of the circuit configuration, it is possible by an external measurement technique to obtain the loop gain characteristics of an amplifier. The only requirement necessary for this technique to be valid is that there be feedback connected to one of the output terminals. This is typical, since low output impedance and gain stability are desired and achieved by this feedback connection.

F. The stability performance of a servo amplifier/servomotor combination can be established by a worst-case stability dummy load test.

G. The power output capability of a servo amplifier can be established by a worst-case power dummy load test.

H. A nominal worst-case dummy load can be established for evaluating servo amplifier phase shift, gain magnitude, gain linearity, and saturated output voltage by means of transfer function plots.

I. A technique is necessary to establish the correlation between the values of  $R_{oc}$  and  $I_s$  and between the values of  $R_s$  and  $I_s$  in order to determine realistic limits for a worst-case dummy load. (See Fig. 3, page 15, for definitions.)

J. A measurement technique was necessary to obtain  $R_{oc}$  and  $I_t$ , since these parameters were not specified.

K. The stability of servo amplifiers is very sensitive to proper signal and power ground connections. The large power ground currents must not flow through the input signal ground lead.

L. Proper heat-sinking of a servo amplifier is very important since the amplifier tends toward instability with increasing temperature.

M. The choice of a dummy load for an amplifier depends on the internal circuit configuration and open loop gain characteristics of the amplifier.

## II. RECOMMENDATIONS

### A. DUMMY LOAD USAGE

Servo amplifier procurement should incorporate testing with worst-case dummy loads to establish more accurate and complete amplifier performance data. It is recommended that three separate dummy loads be utilized. A nominal dummy load should be utilized to obtain amplifier room temperature performance data such as gain magnitude, gain linearity, phase shift, and saturated output voltage level.

The second load is the worst-case stability dummy load. This load should represent the worst set of amplifier load parameters which would tend to cause oscillations in the amplifier output voltage. The amplifier should be at high temperature when tested with this load to establish a worst-case stability condition. The dummy load may be designed for use at room temperature by having all its temperature-dependent parameters altered to simulate a motor at the worst-case high temperature.

The third load that should be used is the worst-case power dummy load. All of the temperature conditions and load parameter values should be chosen to provide a load which will produce minimum in-phase power delivered to the load.

It is suggested that the complex motor model (Fig. 5, page 17) be used for the worst-case stability dummy load. The parameters which must have their ranges specified to determine the simpler equivalent series motor model (Fig. 28b, page 65) are  $R_s$ ,  $L_s$ ,  $R_{oc}$ ,  $L_{LP}$ . The coupling coefficient,  $K$ , between the stator and rotor of the servomotor is the only additional parameter needed to obtain the complex model parameters from the equivalent series model data. Preliminary calculations from the limited amount of testing performed indicate that only the value of  $K$  has a secondary effect on the motor impedance ( $Z_{12}$ ) and, consequently, on the stability in the frequency regions where instability is likely to occur. Therefore, it is recommended that only the parameters for the equivalent series motor model ( $R_s$ ,  $L_s$ ,  $R_{oc}$ , and  $L_{LP}$ ) be required on the motor specification. The value of  $K$  should then be determined by the method presented in the report when worst-case dummy loads are being developed.

## B. SERVO MOTOR SPECIFICATION CHANGES

Servomotor specifications should include the maximum value of the leakage inductance between the halves of the control winding ( $L_{LP}$ ) and the range of values of the control winding DC resistance ( $R_{DC}$ ) as defined in Figure 28b, page 65. The technique presented in this report to measure these recommended motor parameters should be utilized.

In order to develop a worst-case dummy load from a motor specification, bounds must be placed on motor parameter values. Using the data available (about 30 samples for each size motor), bounds were placed on the motor parameters. It was observed that realistic bounds could only be established when correlation between certain motor parameters are taken into account. The value of the control winding series reactance ( $X_{LS}$ ) is correlated with the control winding total series resistance ( $R_s$ ) and DC resistance ( $R_{DC}$ ). Since  $X_{LS}$  is the motor parameter which had the minimum value distribution spread about the sample average, it was chosen as the independent variable for the correlation. Thus, for every value of  $X_{LS}$ , there exist ranges of the values of  $R_s$  or  $R_{DC}$ . The region of acceptable motor parameter combinations on a plot of  $X_{LS}$  versus either  $R_s$  or  $R_{DC}$  would be a parallelogram rather than the square region obtained when all parameters are considered to be independent of each other.

It is recommended that similar testing on larger sample sizes be performed to establish more accurate correlation and data spread information for the motors. However, using the limited sample sizes available for this study, specifications for all the motor parameters were determined. The values of  $X_{LS}$  all fell within a range of  $\pm 15\%$  around the sample average. The least squares best linear fit curve was drawn on the plots of  $X_{LS}$  versus  $R_s$  and  $R_{DC}$ . The allowable spread of  $R_s$  and  $R_{DC}$  values for any particular value of  $X_{LS}$  was assumed to be  $\pm 15\%$  (of  $R_s$  and  $R_{DC}$  sample averages) around the best linear fit curves. Table I provides the coordinates of the corners of the parallelograms defining regions of acceptable motor parameters on the  $X_{LS}$  versus  $R_s$  or  $R_{DC}$  plots. The equations for the least squares best linear fit correlation relationships

NAFI TR-1331

between parameter data sets are given in Table II. Out of the total of 80 motor data sets available, only the data for two motors did not fall within the parallelograms.

In addition to specifying  $X_{ls}$ ,  $R_s$ , and  $R_{oc}$  using correlation techniques, the maximum value of the leakage inductance between the halves of the control winding ( $L_{lp}$ ) should be specified. The largest value of  $L_{lp}$  is the worst-case as far as stability is concerned, and  $L_{lp}$  does not significantly affect the nominal or worst-case power dummy loads at 400 Hertz. A worst-case value of 2.6 mh was used to determine the dummy loads for the set of motors investigated. This value was slightly higher than the highest experimental value which was 1.8 mh.



**TABLE I** Coordinates of the Corners of the Parallelograms  
Defining Regions of Acceptable Motor Parameter Combinations

Motor Size	$X_{ls}$ (Ohms)	$R_{dc}$ Range* (Ohms)	$R_s$ Range (Ohms)
8	160.6	64.3 - 91.1	96.9 - 141.7
	217.3	87.3 - 114.1	157.7 - 202.5
11	151.5	17.4 - 27.2	49.7 - 85.7
	205.0	37.9 - 47.7	157.6 - 194.2
15	81.7	6.8 - 10.6	33.5 - 51.3
	110.5	14.9 - 18.7	67.6 - 85.4

\* $R_{dc}$  measured at room temperature

**TABLE II** Least Squares Best Linear Fit Equations

Motor Size	Equations for Least Squares Best Linear Fit
8	$E_{dc} = 0.4057(X_{ls}) + 12.536$
8	$R_s = 1.0732(X_{ls}) - 53.083$
11	$R_{dc} = 0.3824(X_{ls}) - 35.625$
11	$R_s = 2.0296(X_{ls}) - 240.136$
15	$R_{dc} = 0.2790(X_{ls}) - 14.074$
15	$R_s = 1.1861(X_{ls}) - 54.529$

### III. INTRODUCTION

#### A. STATEMENT OF PROBLEM

The basic problem and purpose of this report is best demonstrated by the following real life example. A servomechanism is designed and tested with a certain servo amplifier/servomotor combination in the control loop. The servo operates satisfactorily and meets all of the design specifications. Specifications are then drafted for the amplifier and motor and sent to manufacturers for bid. The contracts for the servo amplifiers and servomotors are awarded respectively to Company A and Company B. The system operates satisfactorily with this particular amplifier/motor combination. Upon completion of the original contract, the servo components are resubmitted for bid. Company C is awarded the contract for the servo amplifiers and Company B retains the contract for the servomotors. When this motor is connected to the amplifier, oscillation occurs. The oscillation normally occurs at some frequency above the specified operating frequency. This, of course, causes extremely expensive production delays and crash analysis studies to determine the cause of the problem.

This example problem points out the fact that present servomotor/servo amplifier specifications are not sufficient to insure the stable operation of amplifier/motor combinations. A sufficient set of specifications were established for the determination of amplifier/motor compatibility. In determining these specifications, the economics of increasing the price of the components due to additional specifications was kept in mind. Therefore, it was of prime consideration to keep the number of additional specifications to a minimum and to establish a testing technique which would not be costly in an inspection and production environment. The following ideas, reasonings, and solutions were used to develop a criterion which would insure the stable operation of servo amplifier/servomotor combinations. It is intended that the information contained in this report will be useful to both manufacturers and users of servo amplifiers and servomotors.

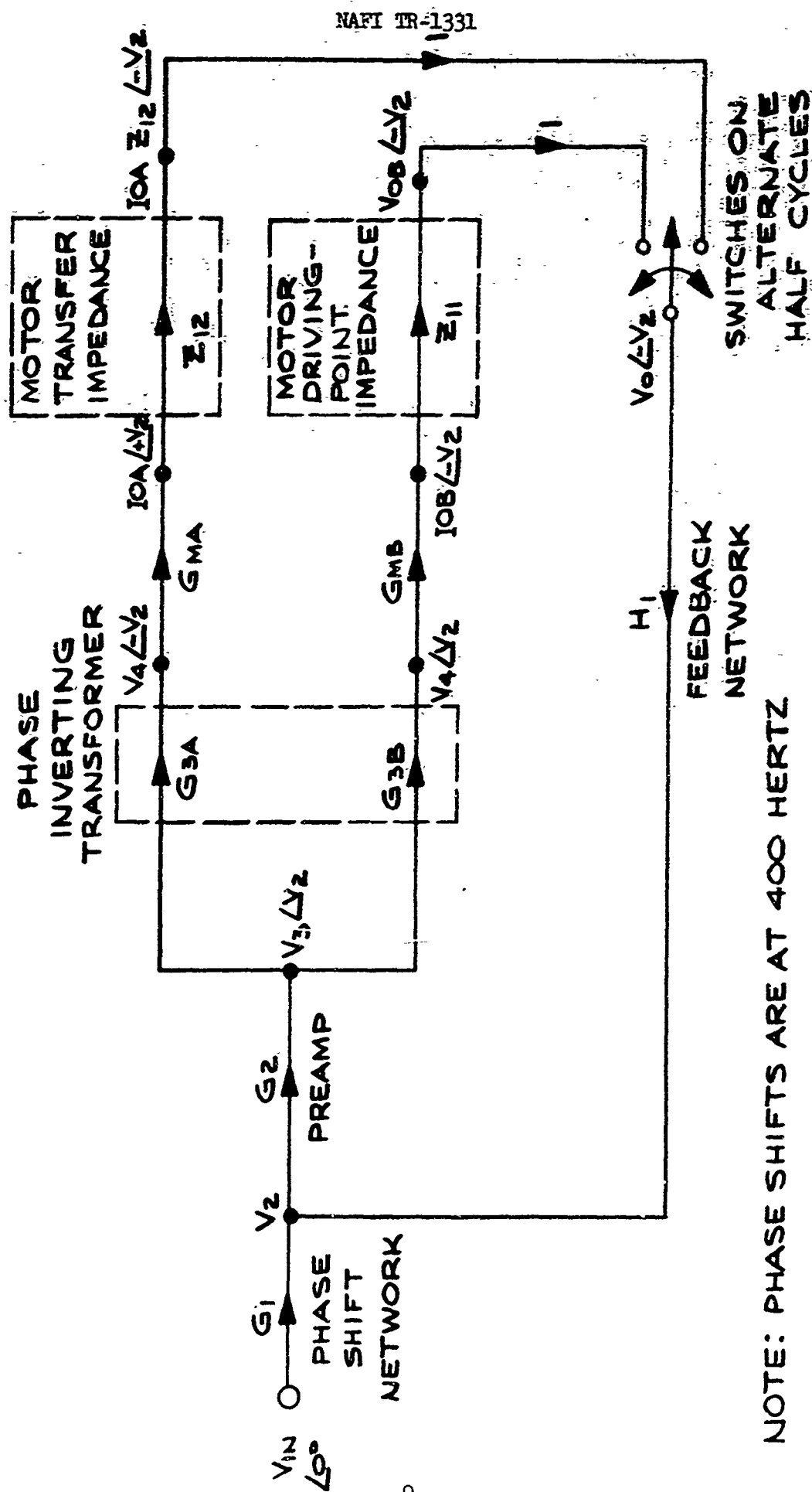
## B. GENERAL DESCRIPTION OF SERVO AMPLIFIER/SERVOMOTOR OPERATION

Figures 1a and 1b illustrate typical servo amplifier/servomotor diagrams for an amplifier with a built-in  $90^\circ$  phase shift. A push-pull, usually Class B, output stage is employed. This type amplifier acts like two separate amplifiers operating on alternate half cycles of the carrier signal, with loop gains that are relatively independent of one another. The stability problem is due to the feedback required to obtain the desired amplifier characteristics of low output impedance and calibrated gain. The feedback loop is normally connected to one side of the output stage, and therefore, has different paths during different half-cycles of the carrier signal. It should be noted that the tuned motor load and the tuned interstage transformer are usually in the feedback loop.

Optimum performance and power transfer to the motor are attained by tuning the motor impedance for unity power factor at the carrier frequency. This is usually accomplished by a parallel tuning capacitor on the control winding. Although some stability advantage can be achieved with a parallel tuning capacitor on each half of the control winding (reference NAFI TR-1053), the continuing efforts toward small size and weight in military electronics favors the single capacitor tuning method. All motor tuning referenced in this report will mean single capacitor tuning unless otherwise specified.

The major consideration in this study is the determination of amplifier/motor compatibility with respect to stability. The advantages and disadvantages of the test methods are reviewed with respect to feasibility for use in a production environment.

A number of amplifiers and motors were tested to verify the theory presented. The results are given in Chapter VIII.



NOTE: PHASE SHIFTS ARE AT 400 HERTZ

FIG. 1a- SERVO AMPLIFIER FLOW GRAPH

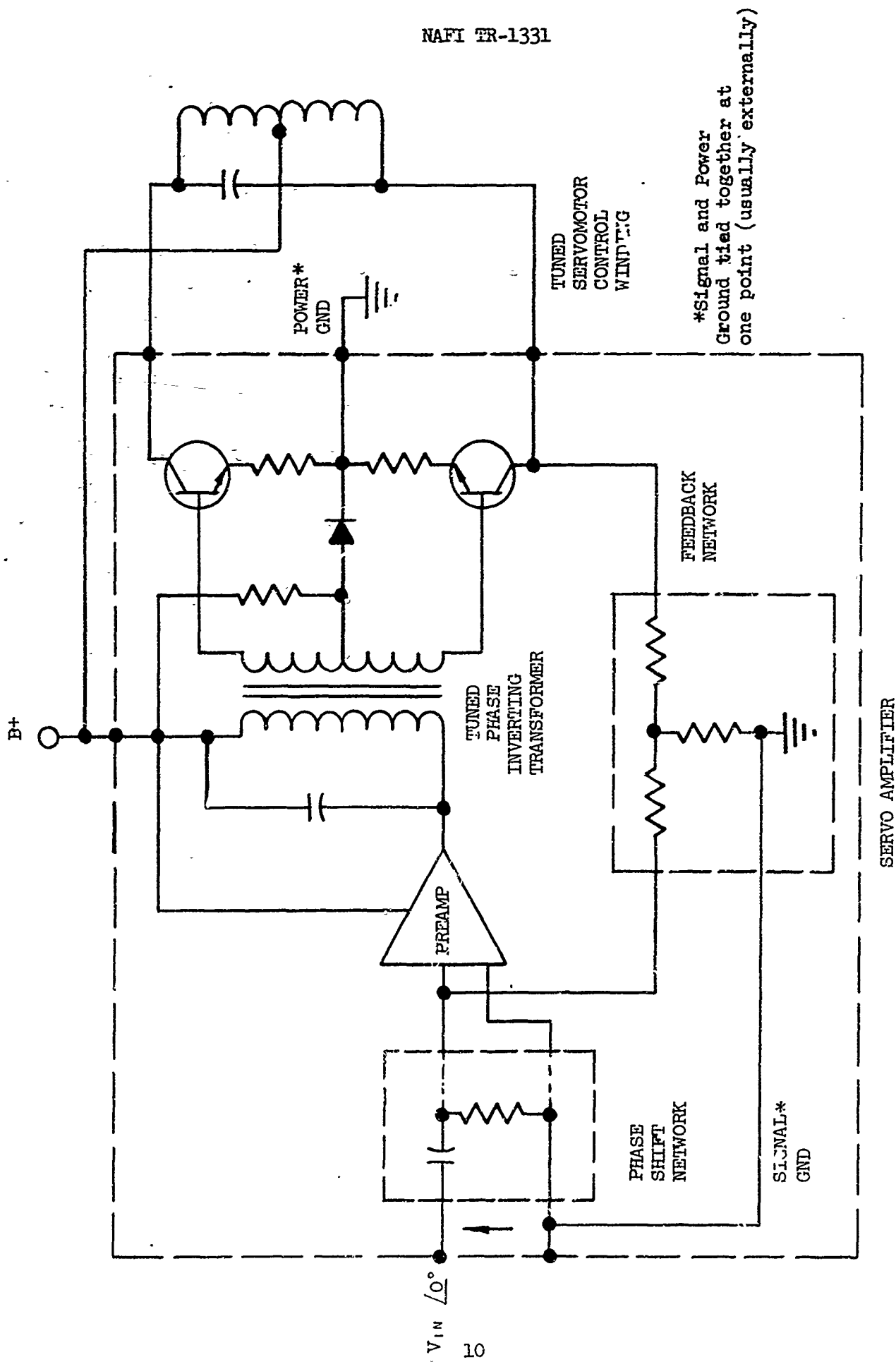


Figure 1b Servo Amplifier Simplified Schematic

IV. SERVO AMPLIFIER/SERVOMOTOR COMPATIBILITY WITH RESPECT  
TO SPECIFICATIONS AND PRODUCTION TESTING

As pointed out in the introduction, present servo amplifier/servomotor specifications are not sufficient to predict the stability performance of the combination. Present servo amplifier specifications state that the amplifiers are designed to operate into an effective impedance of XXX (ohms). This specification assumes that the load is basically inductive and tuned at the operating frequency by means of a parallel tuning capacitor. The specification in no way takes into account the stability characteristics of the amplifier over the entire frequency range of interest.

Present servomotor specifications call out nominal values of the series resistive component of the complex impedance ( $R_s$ ) and the series reactive component of the complex impedance ( $X_{Ls}$ ). These specifications are sufficient to specify a motor model that adequately simulates the characteristics of a servomotor at the operating frequency. It shall be demonstrated that a stability problem does not exist at the operating frequency, but at some value above the operating frequency. Because of this fact, the present servomotor specifications and models are not adequate to properly simulate the characteristics over the entire frequency range of interest.

The first consideration in determining stable operation of the amplifier/motor combination is to establish a method to predict the stability characteristics of the servo amplifier. In order to predict the stability performance, it is necessary to obtain the open-loop gain characteristics of the amplifier. The first method utilized consisted of performing a circuit analysis using the NAFI CODED (Computer Oriented Design of Electronic Devices) circuit analysis program on the amplifier/motor combination. This technique is not feasible in a production environment because the amplifier manufacturers are hesitant to release the actual circuit schematics which are of a proprietary nature. Even if the schematics were available, there is no guarantee that the manufacturer

will not change the circuit configuration in the middle of the contract so as to improve the circuit design and performance. For these reasons, this method of obtaining open-loop gain characteristics is not satisfactory in a production environment.

The second method of obtaining the open-loop gain characteristics of the amplifiers consists of obtaining a frequency response of the amplifier with the feedback loop opened. This method is also not feasible in a production environment since the amplifiers are totally encased and usually have no access to the feedback loop.

Since the amplifier internal circuitry cannot be determined nor usually specified, and since there is no access to the feedback loop, it is necessary to look at the characteristics of the amplifier from terminal (external) measurements. In general, any circuit with one or more feedback loops can be represented by an equivalent circuit with only one feedback loop. The equivalent circuit utilized in this study is illustrated in Figure 2. The parameters  $G$ ,  $H$ , and open-loop output impedance ( $Z_o(OL)$ ) are frequency dependent variables. Usually  $Z_o(OL)$  is high compared to the load impedance and is neglected.

A method was devised to measure the  $GH$  product as a function of frequency and is presented in Chapter VI. From the values of the  $GH$  magnitude and angle at each frequency, a load could be calculated that would cause instability ( $GHZ_L = \text{loop-gain} = 1 / 180^\circ$ ). The plot of this critical load versus frequency is then compared with a plot of the motor load as a function of frequency (see Figure 21).

From a comparison of the two plots, it can be determined whether this particular motor load can cause instability. A more thorough dissertation of this testing method and stability criteria is given in Chapter VI. As a method of insuring the stable operation of amplifier/motor combinations, this method is not feasible. A large amount of time and effort is required to obtain the frequency characteristics of each individual amplifier. However, this method of obtaining the open-loop gain characteristics is valuable and necessary to determine a worst-case dummy load which can be used to test amplifiers. It is also useful in

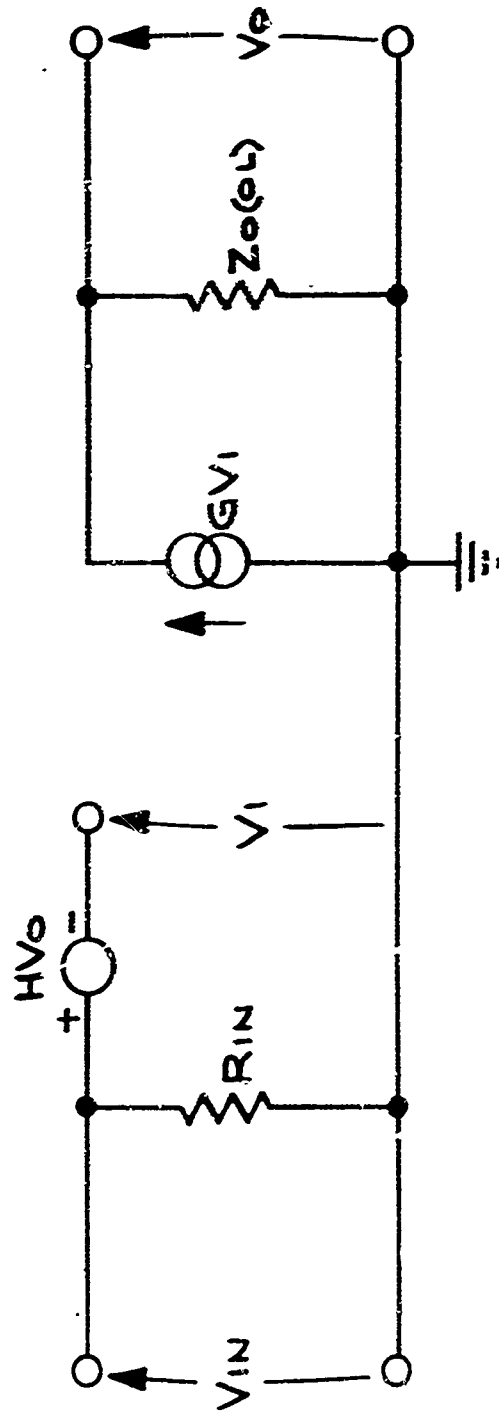


**FIG 2 SERVO AMPLIFIER EQUIVALENT CIRCUIT**



the design of servo amplifiers. From the standpoint of specifications, this method would require the specification of limits for open-loop gain characteristics which would be difficult to check in the incoming qualification of amplifiers.

The method suggested for specifying and testing production amplifiers and motors for compatibility is called the worst-case stability dummy load test method. Either by means of previous experience or by means of obtaining the open-loop characteristics of a sample of amplifiers, the general open-loop gain characteristics of the amplifiers must be known. With this knowledge, a proper selection of servomotor parameters can be made which will result in a worst-case stability dummy load. This load is effectively the worst load with respect to stability to which the amplifier may be subjected. Each amplifier may be tested with this specified dummy load to insure stable operation with a specific size of motor over an entire frequency range. The only necessary addition to present amplifier specifications is to include testing the amplifier with the worst-case dummy load.

In order to properly determine a dummy load which will simulate the servomotor characteristics over the frequency range of interest, a more thorough servomotor specification is necessary. The additional specifications required include a tolerance on  $R_s$  and  $X_{ls}$ , the DC resistance ( $R_{dc}$ ) with an appropriate tolerance, and the maximum value of the leakage inductance ( $L_{lp}$ ). Justification for the addition of these parameters lies in the requirement for a more accurate motor model. Chapters V and VII and NAFI TR-1053 validate the necessity of an improved motor model.

Economically speaking, the dummy load method of testing with the addition of these few parameters is the best approach. The justification for the increase in price for the addition of these specifications of course reverts back to the savings that will result due to reductions of production shut-downs caused by the stability problem. Normally, when the stability problem occurs, an analysis of the problem results which can also add an appreciable amount to the already high cost of the shut-down.

## V. SERVOMOTOR DISCUSSION

### A. SERVOMOTOR DESCRIPTION

#### 1. Equivalent Circuits

Servomotor manufacturers' specifications list the equivalent series circuit parameters as shown in the equivalent series motor model of Figure 3.

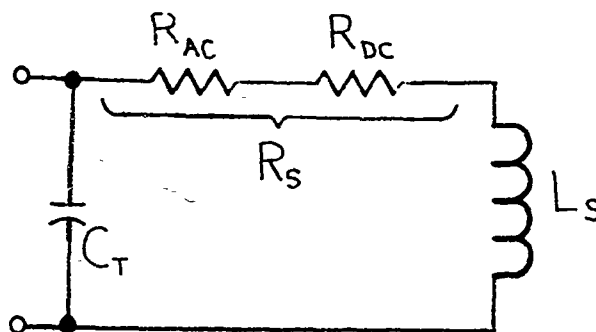


Figure 3 Equivalent Series Motor Model

The inability of this series circuit to properly simulate actual motor impedance over the frequency range of interest necessitates the use of a more complex servomotor equivalent circuit. Most literature uses the simplified equivalent circuit shown in Figure 4 to represent one phase of a servomotor operating under balanced conditions. However, servomotors with center-tapped control winding for push-pull amplifier applications suggest an equivalent circuit with three input terminals. Actual servo amplifier operation as shown in Figure 1 further justifies this idea. Therefore, Figure 5, the modified servomotor equivalent circuit as suggested in NAFI TR-1053, is the choice for most practical applications with balanced input motor voltages. In a null-type servo system, the voltage on the control phase will be much less

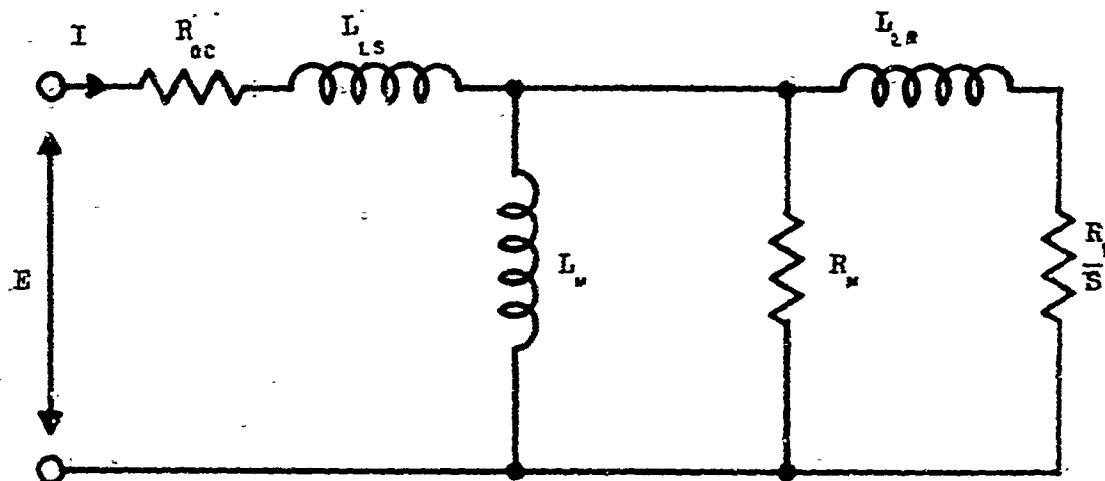


Figure 4 Complex Equivalent Circuit of the Servomotor

SYMBOL = SERVOMOTOR PARAMETER

$R_{ac}$  = Stator copper loss

$L_{ls}$  = Stator leakage inductance

$L_{lr}$  = Rotor leakage inductance

$L_m$  = Magnetizing inductance

$R_m$  = Core loss

$R_r$  = Rotor resistance

$S$  = Slip

$\frac{R_r}{S}$  = Effective rotor resistance

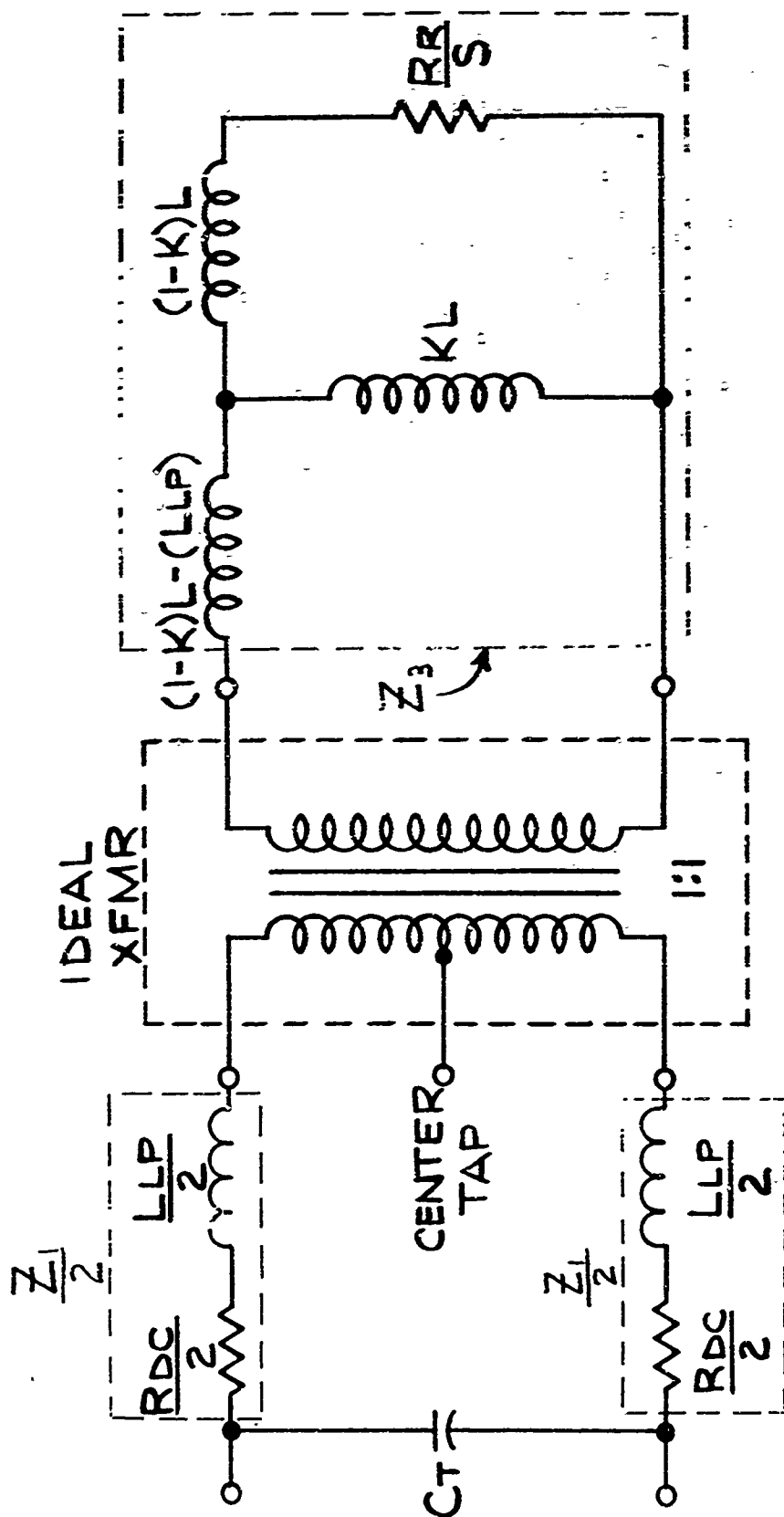


FIG. 5 IDEAL DUMMY LOAD FOR THE COMPLEX MOTOR MODEL

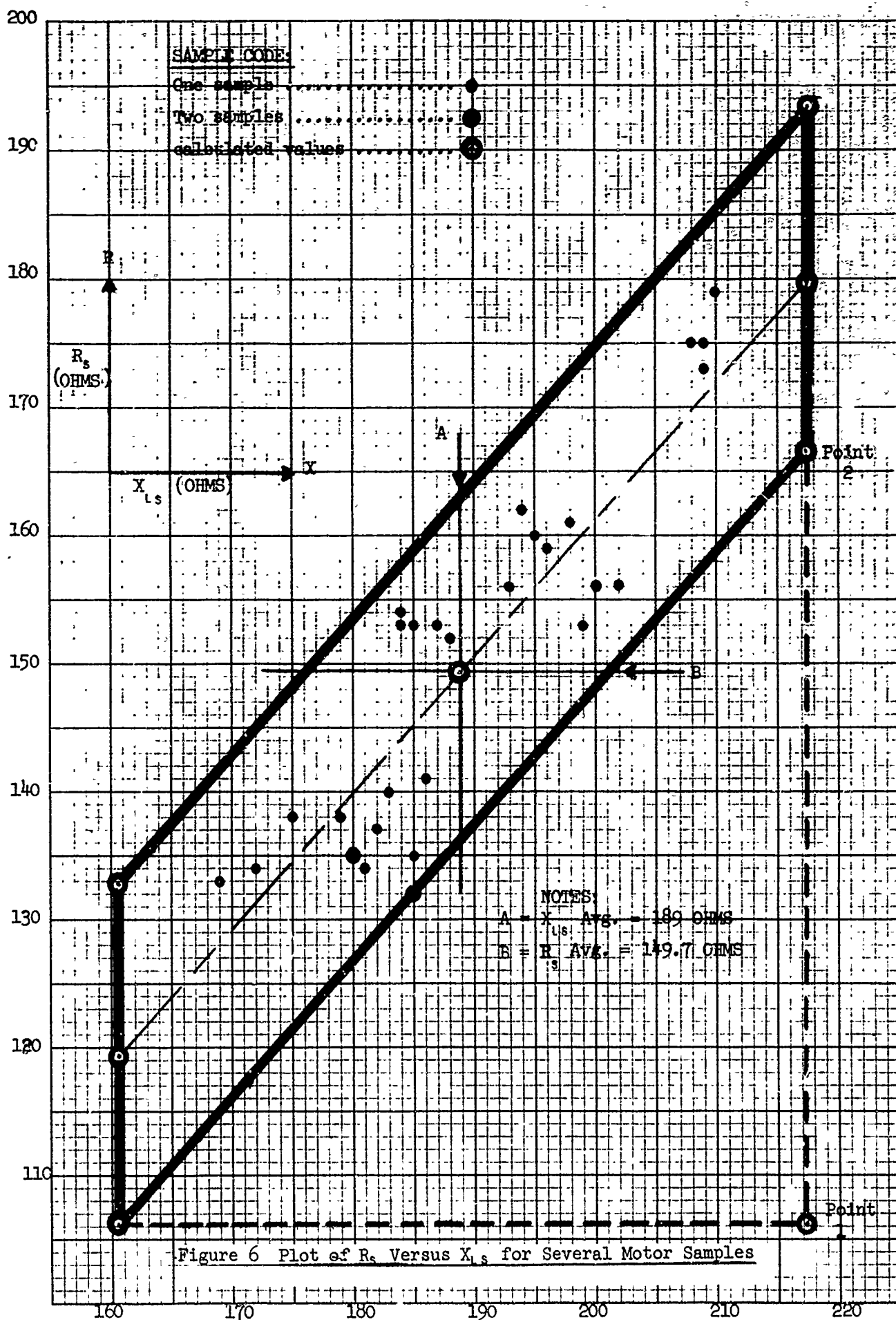
than the rated value a large percentage of the time. However, an analysis of the loads for an unbalanced and a balanced case, using the CODED circuit analysis computer program, resulted in little significant difference between the loads at frequencies away from 400 Hz.

## 2. Equivalent Circuit with Center-Top Control Winding

In Figure 5, the control phase winding DC resistance ( $R_{oc}$ ) and the leakage inductance ( $L_{Lp}$ ) between the halves of the control winding are shown in the primary circuit of an ideal transformer. This transformer is necessary to reflect the load to either half of the control winding depending on which half of the amplifier output is operating. The symmetric transformer equivalent simulates the stator and rotor loading in the secondary as follows: The magnetizing inductance and the stator and rotor leakage inductances are represented in terms of the coupling coefficient ( $K$ ) between stator and rotor windings.  $R_R/S$  is the effective resistance of the rotor. Note that the iron magnetization losses represented by resistance  $R_m$  in Figure 4 are ignored. According to most sources, this is a fair approximation since the ratio of  $R_m$  to  $X_{LM}$  is much greater than one. The impedance groups of  $Z_1$  and  $Z_2$  are utilized in the procedure to determine the equivalent circuit parameters.

### B. EQUIVALENT SERIES CIRCUIT PARAMETER CORRELATION

In order to specify worst-case dummy loads, the servomotor parameters must have limits associated with each of them. Initially, the motor parameter limits were established and a dummy load developed, based on the assumption that all motor parameters were independent of each other. However, nearly every amplifier tested with this load exhibited unstable operation. After further investigation, it was determined that there is correlation between the  $R_{oc}$ ,  $R_s$ , and  $X_{Ls}$  motor parameters, and this was not considered in the initial dummy load. The result was that the dummy load parameters were placed at their uncorrelated extremes in such a way that actual motor parameter data would not come close to the dummy load data. For example, consider the plot of  $R_s$  versus  $X_{Ls}$  for several motor samples as illustrated in Figure 6. It was determined that the condition where  $X_{Ls}$  is maximum and  $R_s$  is minimum is the worst case as far as stability is concerned. The uncorrelated parameter specifications would have indicated the use of data corresponding



to point 1 (Figure 6) while all of the data fell within the parallelogram indicated by the heavy lines. Actually, the data at point 2 represents a much more realistic worst-case set of data for dummy load determination.

The simple series equivalent circuit of the servomotor was used because a large part of the experimental data available for this study consisted of data for the simple case only. Most of the actual motors were not available for further testing, so all data correlation and distribution information had to be derived from the series equivalent circuit. The servomotors for which data was available are listed in Table III. Table IV lists the series equivalent circuit parameters received from Kearfott and NAD, Crane, Indiana. Table V gives the series equivalent circuit parameters and the complex equivalent circuit parameters for the servomotors tested at NAFI. As it will be pointed out later, the worst-case dummy load was first determined in terms of the series circuit parameters and then converted to the more complicated equivalent circuit (Figure 5) for experimental testing.

Excluding temperature variations, the DC resistance ( $R_{0c}$ ) in properly wound motors is dependent only upon type, size, and length of the control winding wire. However, actual sample tests on 30 motors revealed worst-case variations of +45% and -30% from the sample average. The value of tuning capacitor (C) is determined by the value of the inductive reactance ( $X_{Ls}$ ) at the design carrier frequency. The variation in value of the leakage inductance ( $L_{Lp}$ ) is mostly due to internal design and manufacturing process. In contrast to the smallness of  $L_{Lp}$  and its control,  $L_s$  is much larger and more controllable. In fact, laboratory tests on motors with consecutive serial numbers from a given manufacturer generally have less than ten per cent variations in  $X_{Ls}$ . Many have variations of less than one per cent. Laboratory tests on sizes 8, 11, and 15 motors from seven manufacturers revealed that each of the approximately 30 motors per size exhibited an  $X_{Ls}$  value within  $\pm 15\%$  of their respective sample average. However, the same tests indicated that the  $R_{0c}$  value fell within the range of -30% to +46% of the sample average. At the same time, the worst-case values of  $R_s$  had a 72% (of sample average) spread.

TABLE III Servomotors

NOTE: THE NUMERICAL PART OF THE IDENTIFICATION CODE DESIGNATES THE MOTOR SIZE.

IDENTIFICATION CODE	MANUFACTURER	MODEL NO.	SERIAL NO.
8A	KEARFOTT	2474474	Y
8B	"	"	Z
8C	VERNITRON	8SM4-12R	2
8D	KEARFOTT	2474474	1
8E	"	"	2
8F	"	"	3
8G	"	"	4
8H	"	"	5
8I	"	"	6
8J	"	"	7
8K	"	"	8
8L	MCMASTERS	26V-08SM4a	00005
8M	"	"	00001
8N	"	"	00002
8P	"	"	00004
8Q	WESTON-TRANS.	"	3421-1
8R	"	"	3421-2
8S	"	"	3421-3
8T	"	"	3421-4
8U	VERNITRON	"	1X
8V	"	"	2X
8W	"	"	3X
8X	"	"	4X
8Y	IMC	"	1
8Z	"	"	2
8AA	"	"	3
8BB	"	"	4
8CC	HAROWE	"	5
8DD	"	"	6
8EE	"	"	9
8FF	"	"	10
11A	KEARFOTT	2474475	A
11B	"	"	B
11C	"	"	C
11D	TACHTRONIC	"	105
11E	"	"	106
11F	"	"	107
11G	KEARFOTT	2474475	1
11H	"	"	2
11I	"	"	3
11J	"	"	4
11K	"	"	5
11L	"	"	6
11M	"	"	7



TABLE III Servomotors (continued)

IDENTIFICATION	MANUFACTURER	MODEL NO.	SERIAL NO.
11N	KEARFOTT	2474475	8
11P	MCMASTERS	11SM4C	00001
11Q	"	"	00002
11R	"	"	00003
11S	"	"	00005
11T	WESTON-TRANS.	"	3421-7
11U	"	"	3421-8
11V	"	"	3421-9
11W	"	"	3421-10
11X	IMC	"	1
11Y	"	"	2
11Z	"	"	3
11AA	"	"	4
15A	KEARFOTT	2474476	7
15B	"	"	8
15C	TACHTRONIC	"	102
15D	"	"	103
15E	KEARFOTT	247447	1
15F	"	"	2
15G	"	"	3
15H	"	"	4
15I	"	"	5
15J	"	"	6
15K	"	"	7
15L	"	"	8
15M	HAROWE	15SM4d	17
15N	"	"	18
15P	"	"	20
15Q	"	"	21
15R	WESTON-TRANS.	"	3421-13
15S	"	"	3421-14
15T	"	"	3421-15
15U	"	"	3421-16
15V	IMC	"	1
15W	"	"	2
15X	"	"	3
15Y	"	"	4

TABLE IV Servomotor Equivalent Series Circuit Parameters Obtained from  
Kearfott\* and NAD\*\*, Crane, Indiana

IDENTIFICATION CODE	$X_{Ls}$ (OHMS)	$R_s$ (OHMS)	$R_{bc}$ (OHMS)	$R_{Ac}$ (OHMS)
8D	179.3	138.1	79.9	58.2
8E	180.0	135.0	79.5	55.5
8F	202.2	155.7	85.8	69.9
8G	182.2	136.7	79.3	57.4
8H	184.8	135.3	79.3	56.0
8I	185.2	132.1	78.8	53.3
8J	185.2	132.1	77.1	55.0
8K	180.0	135.0	79.6	55.4
8L	193.8	161.8	87.6	74.2
8M	195.6	159.2	89.4	69.8
8N	198.4	160.5	89.4	71.1
8P	198.7	153.2	88.8	64.4
8Q	184.0	153.5	98.6	54.9
8R	174.5	148.2	101.5	46.7
8S	195.2	160.3	98.0	62.3
8T	193.4	156.0	97.0	59.0
8U	209.1	175.0	102.0	73.0
8V	209.3	172.5	101.4	71.1
8W	208.2	174.6	103.5	71.1
8X	210.4	179.2	102.5	76.7
8Y	168.6	133.3	85.0	48.3
8Z	180.5	134.4	84.5	49.9
8AA	174.7	138.4	85.2	53.2
8BB	172.2	133.5	84.0	49.5
8CC	184.1	152.8	91.0	61.8
8DD	187.1	152.9	90.4	62.5
8EE	187.8	152.0	91.9	60.1
8FF	184.6	153.3	91.9	61.4
11G	175.0	103.7	26.8	76.9
11H	181.0	110.1	26.4	83.7
11I	175.0	103.7	24.7	79.0
11J	170.9	104.0	27.0	77.0
11K	173.2	111.1	27.5	83.6
11L	173.7	105.8	26.6	79.2
11M	172.2	110.4	27.0	83.4
11N	170.9	104.0	27.6	76.4
11P	183.2	112.6	28.5	84.1
11Q	179.4	109.0	28.2	80.8
11R	171.3	97.9	28.4	69.5
11S	175.7	99.0	28.5	70.5
11T	183.1	148.0	37.7	110.3
11U	184.4	149.9	37.7	112.2
11V	186.0	158.7	37.2	121.5

TABLE IV (Continued)

IDENTIFICATION CODE	$X_{L_s}$ (OHMS)	$R_s$ (OHMS)	$R_{D_c}$ (OHMS)	$R_{A_c}$ (OHMS)
11W	186.5	157.2	37.6	119.6
11X	202.3	165.5	43.8	121.7
11Y	204.5	164.3	43.4	120.9
11Z	199.2	162.3	43.0	119.3
11AA	189.4	174.6	44.5	130.1
15E	88.3	53.5	11.2	42.3
15F	89.4	51.5	11.2	40.3
15G	89.1	51.5	11.2	40.3
15H	91.3	50.1	11.3	38.8
15I	90.3	52.2	11.2	41.0
15J	89.1	51.5	11.1	40.4
15K	90.4	52.2	11.2	41.0
15L	88.9	54.2	11.2	43.0
15M	96.7	58.2	12.3	45.9
15N	93.0	60.0	12.4	47.6
15P	95.1	59.7	12.5	47.2
15Q	95.5	61.6	12.4	49.2
15R	97.0	60.2	11.0	49.2
15S	96.7	61.1	10.9	50.2
15T	97.9	62.8	10.9	51.9
15U	97.8	62.6	11.1	51.5
15V	106.4	71.9	16.0	55.9
15W	105.1	70.4	16.4	54.0
15X	104.6	74.6	17.0	57.6
15Y	106.2	72.0	16.3	55.7

\* Bureau of Naval Weapons Contract Number NOW 62-1000-F awarded to Kearfott Division, General Precision, Inc., Little Falls, New Jersey.

\*\* Naval Ammunition Depot

TABLE V									
SERVOMOTOR EQUIVALENT CIRCUIT PARAMETERS FOR MOTORS TESTED AT NAFI									
ID CODE	SERIES EQUIVALENT CIRCUIT				COMPLEX EQUIVALENT CIRCUIT				
	$R_{oc}$ (OHMS)	$R_{Ac}$ (OHMS)	$R_s$ (OHMS)	$X_{Ls}$ (OHMS)	$R_1(R_{oc})$ (OHMS)	$L_1$ (mh)	K	L (mh)	$R_2$ (OHMS)
8A	88	52.3	140.3	182.8	88	1.84	.737	84.5	385
8B	88	67.5	155.5	199.7	88	1.72	.730	87.7	380
8C	86.4	54.1	138.1	186.1	86.4	1.78	.705	85.6	300
11A	28.9	55.6	84.5	168.6	28.9	1.59	.815	83.2	387
11B	28.7	68.2	96.9	171	28.7	1.71	.83	88.4	250
11C	29.3	62	91.3	163.7	29.3	1.59	.823	83.6	310
11D	35.7	76.9	112.6	166.2	35.7	.9	.884	96.6	355
11E	35.7	84.8	120.5	164.2	35.7	.96	.875	92.0	320
11F	36	70.4	106.4	164.5	36.0	.97	.859	89.8	310
15A	12.73	36.77	49.5	91.5	12.73	1.04	.8	44.75	184
15B	12.06	32.64	44.7	91.1	12.33	.84	.779	43.8	185
15C	16.08	53.82	69.9	109.9	16.08	.61	.859	68.8	192
15D	16	54.7	77.7	104.8	16.00	.58	.885	66.75	198

It can be seen from the above parameter spreads, that the parameter most closely controlled and most easily specified is  $X_{1s}$ . It was for this reason that  $X_{1s}$  was chosen as the independent variable in a correlation analysis of the motor parameters. All of the sample values of  $R_s$  and  $R_{pc}$  were plotted versus  $X_{1s}$  as illustrated in Figures 6 and 7 for size 8 motors. The linear least squares fit relationships between each of the sets of data were determined using a library computer program provided by the G.E. time-sharing service. A  $\pm 15\%$  tolerance around the sample average was placed on the value of  $X_{1s}$  since all of the data fell within this range. Lines were then drawn parallel to the best linear fit line and displaced from this line by an amount equal to  $\pm 15\%$  of the  $R_s$  and  $R_{pc}$  sample averages. The resulting parallelogram specifies a much more realistic region in which the sets of parameters of "acceptable" motors must lie. If a motor data set lies outside this region, the stability predicted by the worst-case dummy load cannot be guaranteed. At least 90% of all motors tested for this study fell within the regions specified.

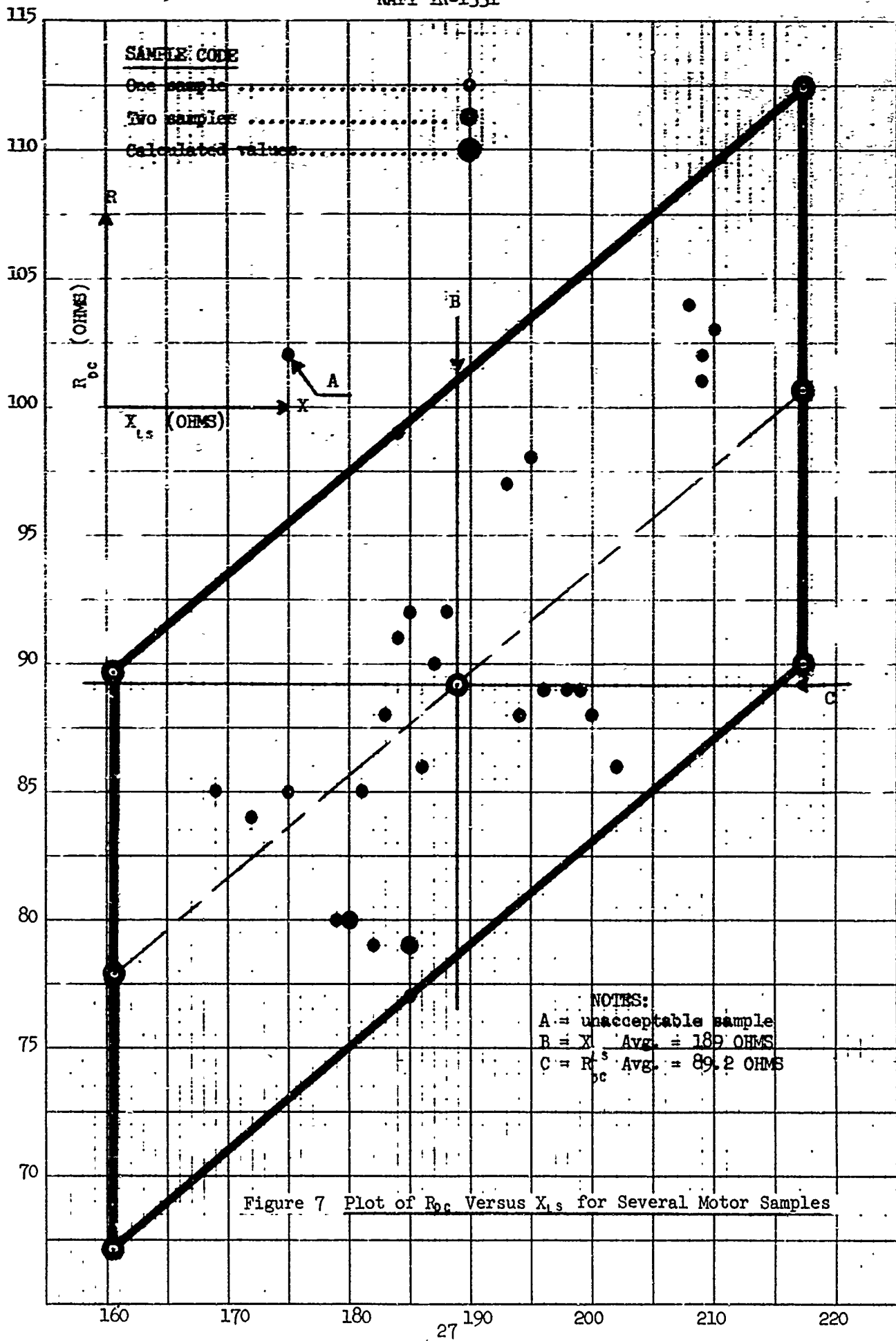
It can be seen that there now exists two values for each of the extremes of  $R_s$  and  $R_{pc}$  corresponding to the maximum and minimum values of  $X_{1s}$ . The sets of data corresponding to the corners of the parallelograms will be used as the parameter extremes necessary for worst-case dummy load determinations.

Figure 8 illustrates a matrix of all the possible worst-case loads.

#### C. COMPLEX EQUIVALENT CIRCUIT PARAMETER DETERMINATION

##### 1. From Experimental Test Results:

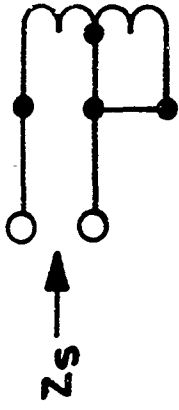
Using measurement techniques as given in NAFI TR-1053,  $Z_0$ ,  $Z_s$ , and  $Z_A$  of the control winding must be measured at various frequencies along the band of interest. These impedances are given in Figure 9 along with their definition in terms of motor impedances  $Z_1$  and  $Z_2$  as previously shown in Figure 5. The values of  $Z_1$  and  $Z_2$  are then calculated for each frequency with the aid of a time-sharing computer program given in Figure 10. A print-out of the results of one of these calculations is given in Figure 11. Note that the print-out provides a check of the data by supplying the measured and calculated values of  $Z_1$  for comparison.



	$R_{dc}$ (MAXIMUM)		$R_{dc}$ (MINIMUM)		
$X_{ls}$ (MAX.)	60*	61	51	50	$R_s$ (MAX.)
$X_{ls}$ (MIN.)	30	31	41	40	
	20	21	11	10	$R_s$ (MIN.)
$X_{ls}$ (MAX.)	70	71	81	80	
	$C_T$ (MIN.)	$C_T$ (MAX.)		$C_T$ (MIN.)	

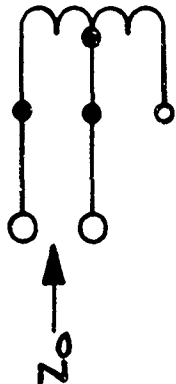
Figure 8 Matrix of Possible Combinations of Extreme Motor Parameters

\*These numbers represent a code for each particular combination of parameters.



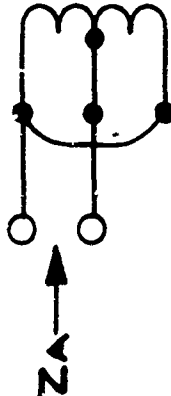
$$Z_s = Z_1 \frac{(Z_1 + Z_3)}{2Z_1 + Z_3}$$

B. SHORT CIRCUIT



$$Z_o = \frac{1}{2} \left( Z_1 + \frac{Z_3}{2} \right)$$

A. OPEN CIRCUIT



$$Z_A = \frac{Z_1}{4}$$

C. ANTIPARALLEL

$$Z_1 = 4Z_A = 2 \left[ Z_o - \sqrt{Z_o(Z_o - Z_s)} \right]$$

$$Z_3 = 4 \sqrt{Z_o(Z_o - Z_s)}$$

$$Z_o \cdot Z_s = 4Z_A(Z_o - Z_A)$$

**FIG.9 SERVOMOTOR IMPEDANCE DETERMINATION**  
(AS SUGGESTED IN NAFI TR-1053)



```

10 REM INSERT DATA IN LINES 1000 TO 2000. THE ORDER OF DATA IS-
20 REM FREQUENCY, VO, VIO, THETA, VS, VIS, PHI, VA, VIA, ALPHA.
100 PRINT "CALCULATION OF SERVO MOTOR IMPEDANCE Z1 AND Z3."
110 PRINT
120 PRINT "ENTER NO. OF FREQUENCIES AND VALUE OF CURRENT SENSING RESISTOR"
130 INPUT N,R1
140 DIM F(15)
150 DIM O(15)
160 DIM S(15)
180 DIM D(15)
190 DIM E(15)
202 PRINT
204 LET K=1
206 PRINT "FREQ","Z1 MAG (MEAS)","Z1 ANG (MEAS)"
210 READ C,VO,V1,A1,V2,V3,A3,V4,V5,A5
220 LET F(K)=C
230 LET O(K)=VO*R1/V1
240 LET S(K)=V2*R1/V3
260 LET D(K)=A1/57.296
270 LET E(K)=A3/57.296
280 PRINT F(K),4*V4*R1/V5,A5
290 LET K=K+1
300 IF K<=N THEN 210
310 PRINT
320 PRINT "FREQ","Z3 MAG","Z3 ANG","Z1 MAG (CAL)","Z1 ANG (CAL)"
330 LET K=1
340 LET Z1=O(K)*COS(D(K))
350 LET Z2=O(K)*SIN(D(K))
360 LET Z3=S(K)*COS(E(K))
370 LET Z4=S(K)*SIN(E(K))
380 LET Z5=SQR((Z1-Z3)^2+(Z2-Z4)^2)
390 LET T5=ATN((Z2-Z4)/(Z1-Z3))
400 IF (Z1-Z3)<0 THEN 420
410 GO TO 460
420 IF (Z2-Z4)>=0 THEN 450
430 LET T5=-3.1416+T5
440 GO TO 460
450 LET T5=3.1416+T5
460 LET Z6=SQR(O(K)*Z5)
470 LET T7=((D(K)+T5)/2)*57.296
480 LET Z7=4*Z6
490 LET Z8=Z6*COS(T7/57.296)
500 LET Z9=Z6*SIN(T7/57.296)
530 LET X3=2*SQR((Z1-Z8)^2+(Z2-Z9)^2)
540 LET T3=ATN((Z2-Z9)/(Z1-Z8))*57.296
550 PRINT F(K),Z7,T7,X3,T3
560 LET K=K+1
570 IF K<=N THEN 340
575 PRINT
580 PRINT "IF MORE DATA NEEDS TO BE PROCESSED, TYPE IN NEW DATA AND"
581 PRINT "RUN AGAIN"
1000 DATA 0
9999 END

```

Figure 10 Time-Sharing Computer Program for Calculation of Motor Impedances  $Z_1$  and  $Z_3$

S-MOTO 15:52 CH-E WE 10/11/7

CALCULATION OF SERVØ MØTØR IMPEDANCE Z1 AND Z3.

ENTER NØ. ØF FREQUENCIES AND VALUE ØF CURRENT SENSING RESISTØR  
? 12,50.25

FREQ	Z1 MAG [MEAS]	Z1 ANG [MEAS]
40	28.8938	3.6
100	28.8938	5.7
200	30.15	10.4
300	30.9038	15.3
400	32.16	18.3
500	34.17	21.7
600	35.6775	24.2
1000	40.7025	31.1
4000	80.4	50.7
10000	145.725	59.7
40000	389.438	69.1
100000	854.25	77.2

FREQ	Z3 MAG	Z3 ANG	Z1 MAG [CAL]	Z1 ANG [CAL]
40	17.9421	42.1675	23.369	11.2639
100	48.7088	82.1075	28.7323	4.48266
200	104.209	78.025	29.4477	10.8801
300	136.673	73.0499	31.661	14.8957
400	167.455	71.2285	32.6309	18.7388
500	200.744	69.6922	33.6832	22.2425
600	227.975	68.5288	34.8347	23.2682
1000	326.425	67.2633	39.8336	28.8
4000	882.042	64.9246	88.9767	50.3961
10000	1856.85	69.271	141.125	59.6089
40000	7073.07	69.7973	383.025	70.8487
100000	19702.6	-42.7853	812.296	79.1365

IF MØRE DATA NEEDS TØ BE PRØCESSED, TYPE IN NEW DATA AND  
RUN AGAIN

TIME: 5 SECS.

Figure 11 Calculated Values of Motor Impedances  $Z_1$  and  $Z_3$

The equivalent circuit parameter values of Figure 5 are calculated from the  $Z_1$  and  $Z_3$  magnitude and angle versus frequency plots shown in Figure 12. From these plots, the significant break frequencies and asymptotic values are obtained. Then, using the equations in Figure 12, the equivalent circuit values are determined.

2. From Mathematical Manipulation of Equivalent Series Circuit Parameters:

Extreme parameter values have been determined for the series equivalent circuit, but the complex equivalent circuit more accurately represents actual motor impedances over the frequency range of interest. To determine which of the 16 possible dummy load configurations (see Figure 8) represents the worst-case stability load, the complex equivalent circuit should be determined and evaluated for each of the 16 possible loads. Areas of probable instability occur at frequencies other than 400 Hz; therefore, the complex circuit is necessary. A comparison of the frequency responses of the two different equivalent circuits is presented in Figure 25b, page 61.

Figure 13 illustrates the two circuits which must be equated at 400 Hz to arrive at parameter values for the complex equivalent circuit. The variables which must be determined are K, L, and R, and the necessary equations are also given in Figure 13. After a value of K is assumed, equation (1) is solved to determine a value of L which is used in equation (2). These equations are solved using a time-sharing computer library program. These equations must be solved several times for different values of K until an acceptable value of K is determined. The preferred values of K (0.6 to 0.9) and R are those close to values obtained on the few motors tested in the lab. In some cases, two values of R are obtained in the allowable range, and the lower value of R is chosen since it is closer to the experimental values obtained.

The results for the servomotors tested at NAFI are given in Table V, page 25.

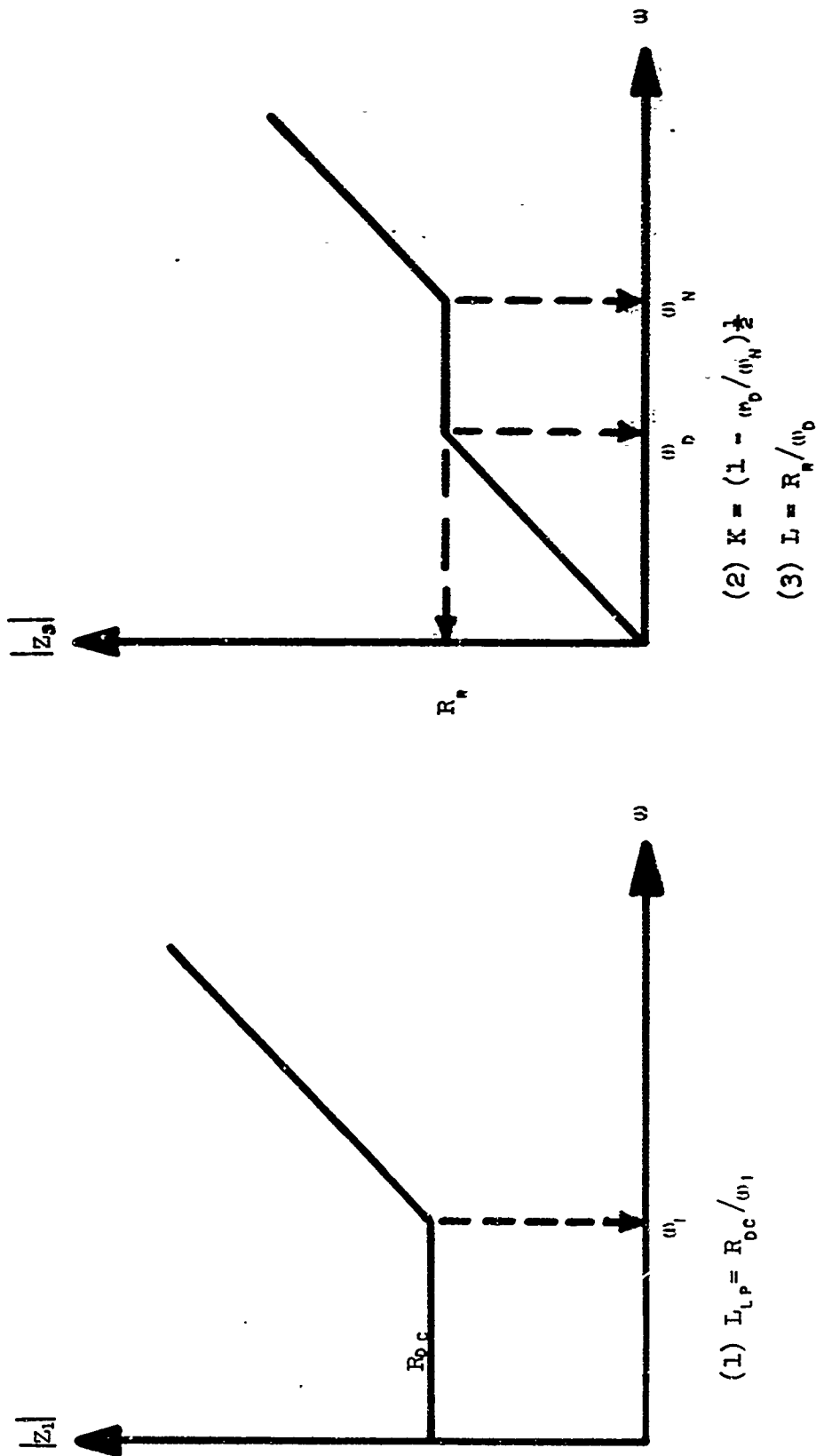
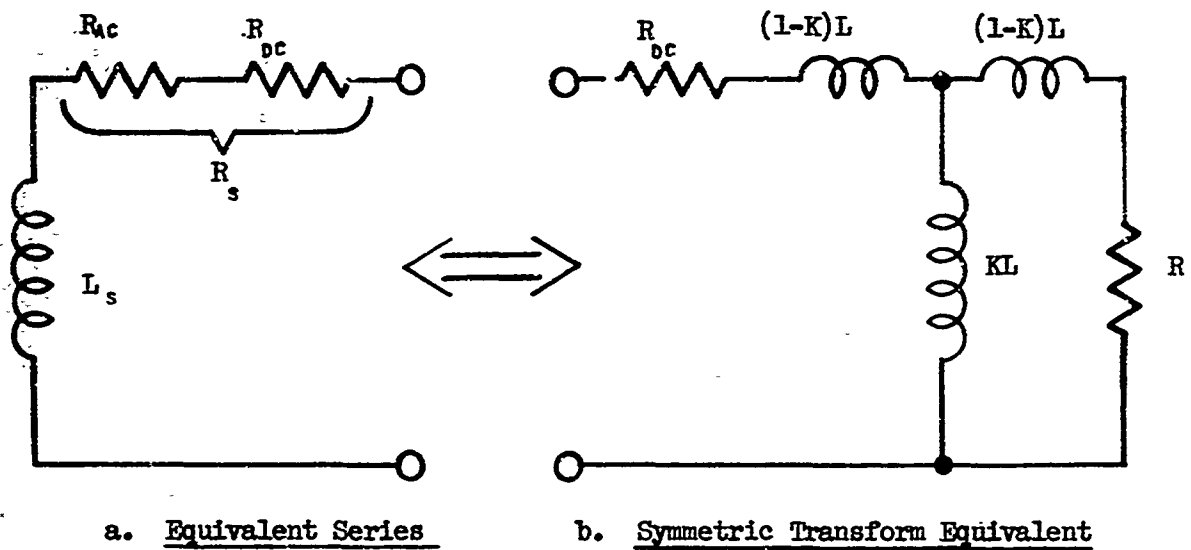


Figure 12 · Bode Plots of  $|Z_1|$  and  $|Z_3|$


EQUATION RESULTS:

$$(1) \quad L^2 = \frac{R^2}{\omega \left[ \frac{K^2 R}{R_s - R_{dc}} - 1 \right]}$$

$$(2) \quad R^2 - \frac{R^2 \omega L}{X_{ls}} + \omega^2 L^2 - \frac{(1-K^2)}{X_{ls}} \omega^3 L^3 = 0$$

Figure 13 Equivalent Servomotor Circuits

A minimum possible value of K can be calculated from the following equation:

$$K_{\min} = \frac{1}{Q_x} \sqrt{2(\sqrt{1 + Q_x^2} - 1)} \quad (5-1)$$

where  $Q_x = \frac{2\pi fL_s}{R_s - R_{oc}}$

The actual value of K chosen has a secondary effect on the motor transfer impedance,  $Z_{12}$ , and consequently, on stability as can be seen in Figure 25b, page 61.

## VI. SERVO AMPLIFIER DISCUSSION

### A. GENERAL DESCRIPTION

The individual representation of motor impedances  $Z_{11}$  and  $Z_{12}$  constitute the motor portion of the servo amplifier/servomotor flow graph shown in Figure 1. The remainder of the flow graph depicts internal amplifier operation. The following equations give the closed loop gain of each half of the amplifier:

$$\frac{V_{0A}}{V_{1N}} = \frac{G_1 G_2 G_3 G_4 Z}{1 - G_1 G_2 G_3 G_4 Z H} \quad (6-1)$$

$$\frac{V_{12}}{V_{1N}} = \frac{G_1 G_2 G_3 G_4 Z}{1 - G_1 G_2 G_3 G_4 Z H} \quad (6-2)$$

From these gain equations, the system characteristic equations are:

$$G_1 G_2 G_3 G_4 Z_{12} H_1 - 1 = 0 \quad (6-3)$$

$$G_1 G_2 G_3 G_4 Z_{11} H_1 - 1 = 0 \quad (6-4)$$

The amplifier/motor combination will oscillate if either equation 6-3 or 6-4 is satisfied. It is obvious that the GH of the amplifier ( $G_1 G_2 G_3 G_4 H_1$ ) is necessary for loop gain calculations. Usually, none of these internal parameter values are available, and it is, therefore, necessary to obtain them by measurements.

In Chapter IV it is pointed out that obtaining the loop gain characteristics by means of CODED analysis or by open-loop frequency

response testing is not feasible in a production environment. Therefore, it is necessary to develop a technique employing external measurement with no access to the feedback loop to determine the internal part of the loop gain.

## B. GH OBTAINED BY EXTERNAL MEASUREMENT

### 1. Equation to Demonstrate Feasibility

It is relatively easy to show how GH may be measured if the circuit has only a single feedback loop. Figure 14 illustrates the flow graph diagram representation of both the closed loop transfer function (C/R) and the impedance measured at the output terminals ( $Z_M$ ) with a load impedance  $Z_L$  attached.  $Z_M$  can be obtained by driving the output terminals with an external current source ( $I_{0x}$ ) and measuring the resulting voltage. The amplifier input terminals are shunted with a resistance equal to that value used as the amplifier source resistance in the servo system.

In the equation for  $Z_M$ , everything except the GH product is known. Figures 15 and 16 illustrate that the same GH measuring technique may also be applied to amplifiers which have multiple or internal feedback loops.

### 2. Measurement Techniques

The GH measurement method consists of obtaining the output impedance of the feedback side of the amplifier over the frequency range of interest. (40 Hz to 100 KHz was used for the laboratory measurements phase of this project.) The circuit utilized is illustrated in Figure 17.

At discrete frequencies in the range of interest, the value of  $R_L$  and the data to compute  $Z_M$  are entered into a computer program to compute GH and the load  $Z_L$  which will make  $GHZ_L = 1/180^\circ$ . This load shall be called  $Z_L$  (unstable). The computer program flow chart is illustrated in Figure 18. Figure 19 presents the computer program as written in G.E. card fortran and Figure 20 presents the computer program as written in time-sharing basic language.



Table VI presents the names of the variables used in these computer programs.

### 3. GH for Non-Feedback Side of the Amplifier

The GH calculated from the output impedance measurements is only for the feedback side of the amplifier (see Figure 1). For the non-feedback side of the amplifier, the absolute value of GH is approximately the same and the phase is  $180^\circ$  from the phase of the feedback side. The value of GH for the non-feedback side cannot be measured by external means.

#### C. HOW TO OBTAIN $Z_{11}$ AND $Z_{12}$ (unstable) CURVES FROM GH CURVES

Since the magnitude of GH is assumed equal for both sides of the amplifier, the magnitude of  $Z_{11}$  or  $Z_{12}$  (for borderline stability) would

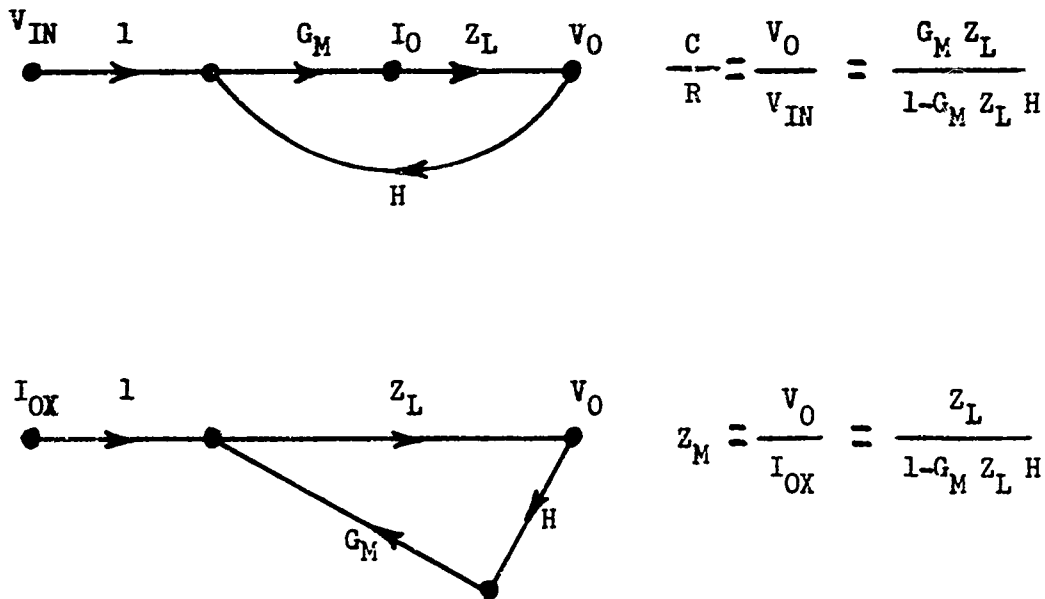
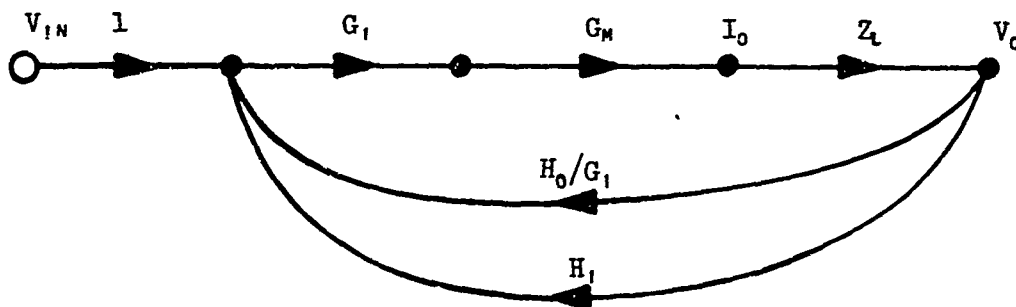
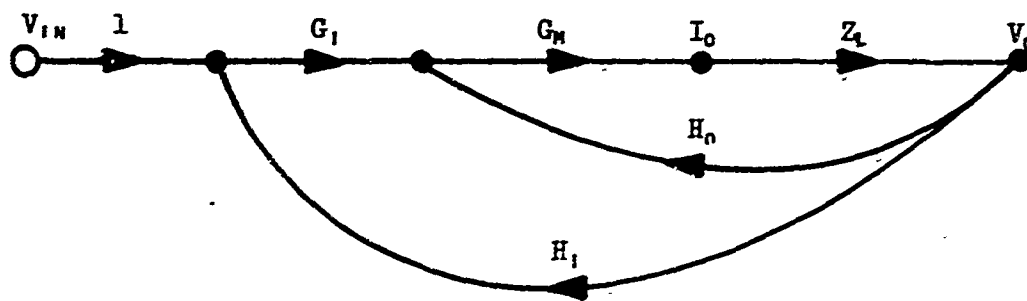
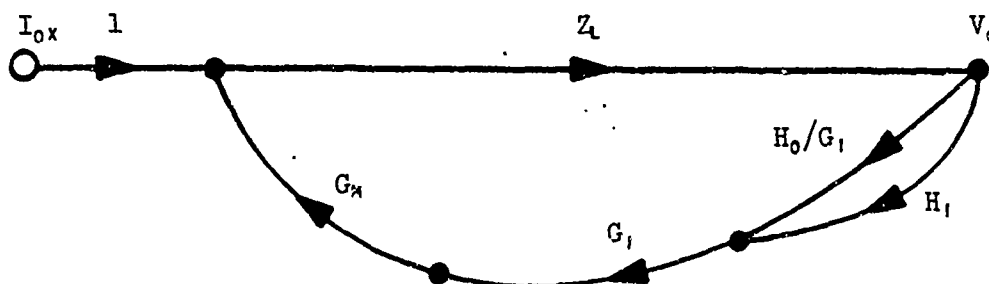


Figure 14 Flow Diagrams of a Single Loop Amplifier

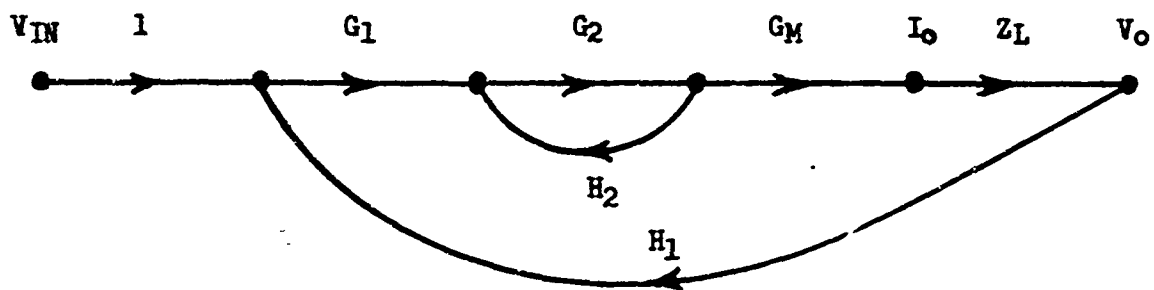


$$\frac{C}{R} = \frac{V_O}{V_{IN}} = \frac{G_I G_M Z_L}{1 - G_I G_M Z_L \left( H_I + \frac{H_O}{G_I} \right)}$$



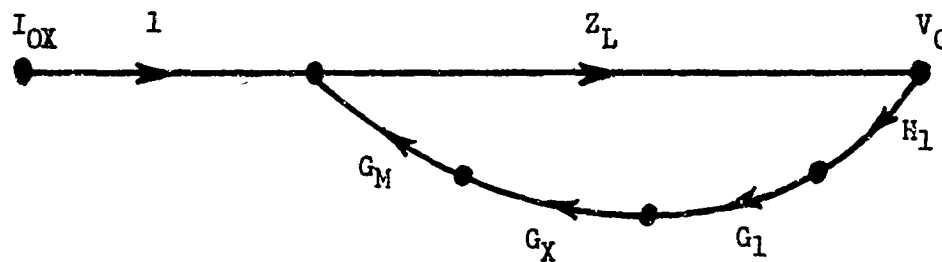
$$Z_M = \frac{V_O}{I_{OX}} \bigg|_{V_{IN} = 0} = \frac{Z_L}{1 - G_I G_M Z_L \left( H_I + \frac{H_O}{G_I} \right)}$$

Figure 15 Flow Diagrams of a Multiloop Amplifier



$$\frac{C}{R} = \frac{V_O}{V_{IN}} = \frac{G_1 G_X G_M Z_L}{1 - G_1 G_X G_M Z_L H_1}$$

$$\text{Where } G_X = \frac{G_2}{1 - G_2 H_2}$$



$$Z_M = \frac{Z_L}{1 - G_1 G_X G_M Z_L H_1}$$

$$\text{Loop Gain} = G_1 G_X G_M Z_L H_1$$

Figure 16 Flow Diagrams of an Amplifier with Internal Loop

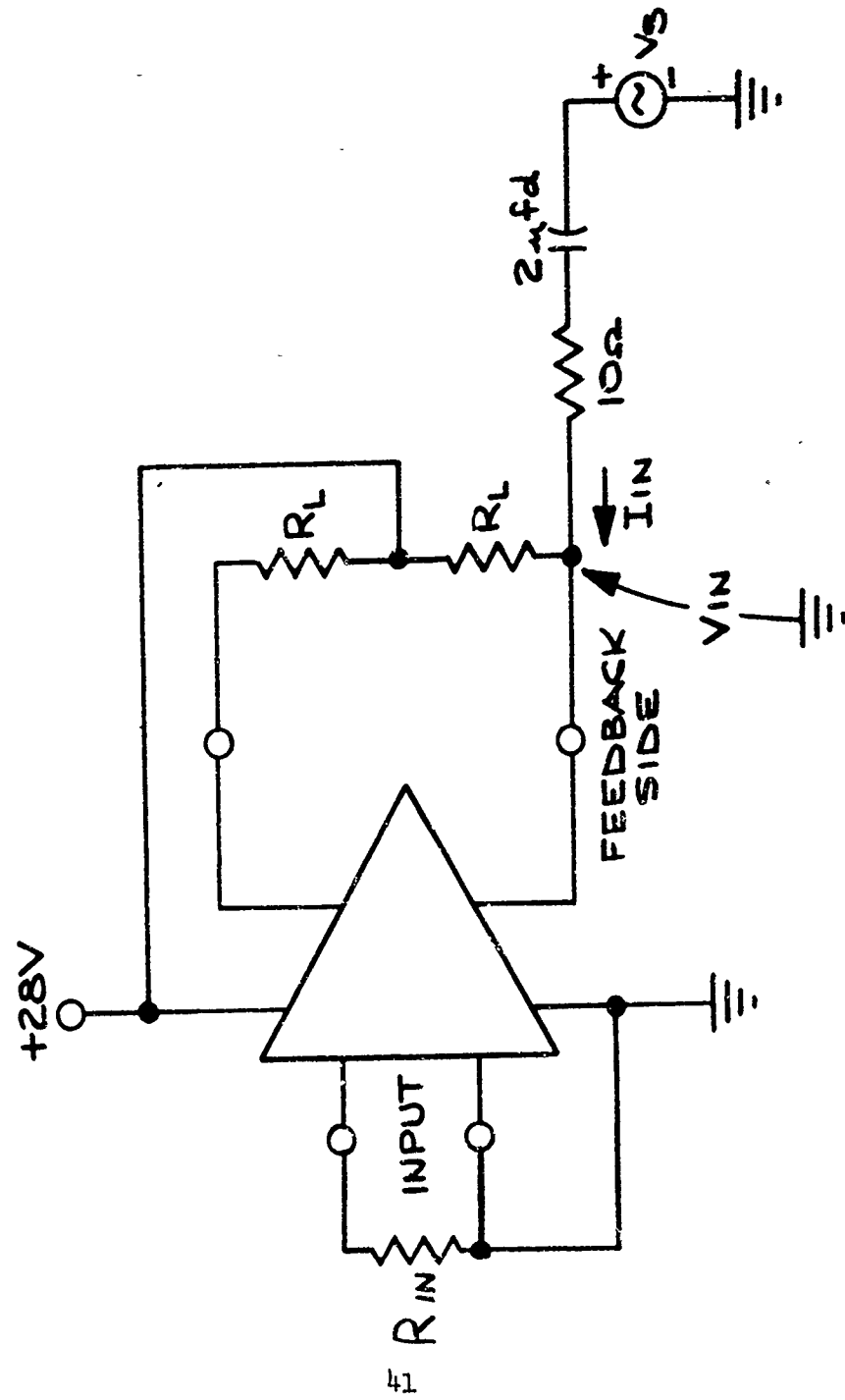


FIG 17 OUTPUT IMPEDANCE MEASUREMENT CIRCUIT

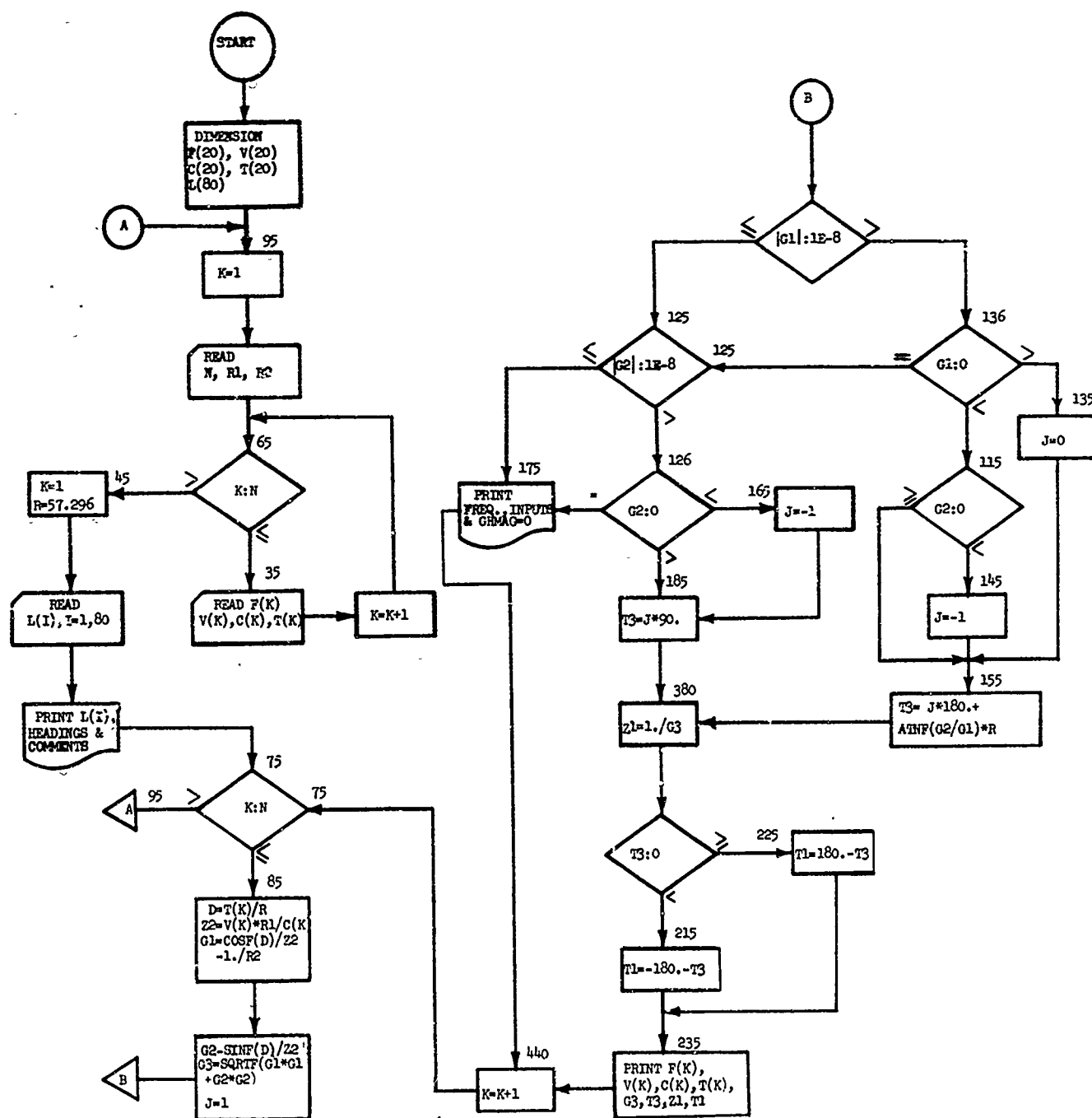


Figure 18 Flow Chart for Computation of GH and  $Z_{unstable}$

NAFI TR-1331

	F03-68-41	GH-EQU	000
	PROGRAM TO CALCULATE GH MAGNITUDE AND ANGLE AND BORDERLINE		100
	STABILITY LOAD. ON FIRST DATA CARD PUT NO OF FREQS(20 MAX), VALUE OF		110
	CURRENT SENSE RESISTOR, AND LOAD RESISTOR VALUE-(FORMAT I3,2F5.0).		120
	ON REMAINING CARDS PUT DATA IN THIS ORDER- FREQ, INPUT VOLTAGE,		130
	CURRENT SENSE VOLTAGE, ANGLE OF INPUT WRT CURRENT SENSE VOLTAGE		140
	-(FORMAT F8.0,3F5.0).		150
	DIMENSION F(20),V(20),C(20),T(20),L(80)		160
95	K=1		170
	READ 25,N,R1,R2		220
25	FORMAT (I,2,2F5.0)		230
65	IF (K-N) 25,35,45		240
35	READ 55,F(K),V(K),C(K),T(K)		250
55	FORMAT (F8.0,3F5.0)		260
	K=K+1		270
	GO TO 65		280
45	K=1		290
	R=57.296		300
	READ 46,(L(I),I=1,80)		302
46	FORMAT (80A1)		304
	PRINT 15,(L(I),I=1,80)		305
15	FORMAT (19H1SA GH CALCULATIONS,/80A1/		306
	1 10H FREQUENCY,7X,3HVIN,10X,3HVCS,		307
	2 6X,11HANG VIN/VCS,4X,6HGH MAG,7X,6HGH ANG,5X,11HZ UNSTB MAG,2X,		308
	3 11HZ UNSTB ANG/)		309
75	IF (K-N) 85,85,95		310
85	D=T(K)/R		320
	Z2=V(K)*R1/C(K)		330
	G1=COSE(D)/Z2-1./R2		340
	G2=-SINF(D)/Z2		350
	G3=SQRTF(G1*G1+G2*G2)		360
	J=1		370
	IF (ABSF(G1)-1E-8) 125,125,136		375
136	IF (G1) 115,125,135		380
115	IF (G2) 145,155,155		390
145	J=-1		400
155	T3=J*180.+ATANF(G2/G1)*R		410
	GO TO 380		420
135	J=0		430
	GO TO 155		440
125	IF (ABSF(G2)-1E-8) 175,175,126		445
126	IF (G2) 165,175,185		450
165	J=-1		460
185	T3=J*90.		470
	GO TO 380		480
175	PRINT 176,F(K),V(K),C(K),T(K)		490
176	FORMAT (4(PE10.4,3X),24HGH MAGNITUDE EQUALS ZERO)		500
	GO TO 440		510
380	Z1=1./G3		520
	IF (T3) 215,225,225		530
215	T1=-180.-T3		540
	GO TO 235		550
225	T1=180.-T3		560
235	PRINT 245,F(K),V(K),C(K),T(K),G3,T3,Z1,T1		570
245	FORMAT (8(PE10.4,3X))		580
440	K=K+1		590
	GO TO 75		600
	END		610

Figure 19 Card FORTRAN Computer Program for Computation of GH and Z<sub>unstable</sub>

```

10 REM INSERT DATA IN LINES 500 TO 800.  THE ORDER OF DATA IS-
20 REM FREQUENCY, INPUT VOLTAGE, CURRENT SENSING VOLTAGE, AND ANGLE
30 REM OF INPUT VOLTAGE WRT CURRENT SENSING VOLTAGE.
100 PRINT "PROGRAM TO CALCULATE GH MAGNITUDE AND ANGLE, AND"
105 PRINT "BORDERLINE STABILITY LOAD"
110 PRINT
120 PRINT "ENTER NO. OF FREQUENCIES, VALUE OF CURRENT SENSE RESISTOR"
121 PRINT "AND LOAD RESISTOR VALUE"
130 INPUT N,R1,R2
140 DIM F(15)
150 DIM V(15)
160 DIM I(15)
170 DIM T(15)
180 LET K=1
190 PRINT
200 PRINT "FREQ","VIN","VCS","PHASE ANGLE OF VIN WRT VCS"
210 IF K>N THEN 250
220 READ F(K), V(K), I(K), T(K)
225 PRINT F(K),V(K),I(K),T(K)
230 LET K=K+1
240 GO TO 210
250 LET K=1
260 PRINT
270 PRINT "FREQ","GH MAG","GH ANG","Z UNSTBL MAG","Z UNSTBL ANG"
280 IF K>N THEN 455
285 LET D=T(K)/57.296
290 LET Z2=(V(K)*R1)/I(K)
300 LET G1=COS(D)/Z2-1/R2
310 LET G2=-SIN(D)/Z2
320 LET G3=SQR(G1*G1+G2*G2)
330 LET J=1
335 IF G1=0 THEN 350
336 IF G1>0 THEN 345
340 IF G2<0 THEN 365
341 GO TO 370
345 LET J=0
346 GO TO 370
350 IF G2>0 THEN 360
351 IF G2=0 THEN 358
355 LET J=-1
356 GO TO 360
358 PRINT "GH MAG EQUALS ZERO"
359 GO TO 440
360 LET T3=J*90
362 GO TO 380
365 LET J=-1
370 LET T3=J*180+ATN(G2/G1)*57.296
380 LET Z1=1/G3
390 IF T3<0 THEN 420
400 LET T1=180-T3
410 GO TO 430
420 LET T1=-180-T3
430 PRINT F(K),G3,T3,Z1,T1
440 LET K=K+1
450 GO TO 280
455 PRINT
460 PRINT "IF MORE DATA NEEDS TO BE PROCESSED, TYPE IN NEW DATA AND "
461 PRINT "RUN AGAIN."
500 DATA 0
999 END

```

Figure 20 Time-Sharing BASIC Computer Program for Computation of GH and Z<sub>unstable</sub>

TABLE VI		
DEFINITION OF VARIABLES USED IN COMPUTATION OF GH AND ZL (UNSTABLE)		
ITEM NO.	VARIABLE	DEFINITION
1	L(I)	User information such as Mfgr., P/N, S/N, etc. (The printout will be a duplicate of the input punched on the final data card.)
2	C(K)	Current sensing voltage array
3	F(K)	Frequency array
4	T(K)	Angle of Input with respect to current sensing voltage array
5	V(K)	Input voltage array
6	D	T(K) in radians
7	G1	Real part of GH
8	G2	Imaginary part of GH
9	G3	GH magnitude
10	N	Number of frequencies
11	R	Conversion factor (radians to degrees)
12	R1	Current sensing resistor value
13	R2	Load resistor value
14	T1	Z1 unstable angle in degrees
15	T3	GH angle in degrees
16	Z1	Z unstable magnitude
17	Z2	Measured impedance at amplifier output



be identical and equal to  $1/GH$ . The angle of  $Z_{11}$ , which would cause borderline stability, is  $180^\circ$  minus the angle of  $GH$ . Also,  $Z_{12}$  has about  $180^\circ$  phase difference from  $Z_{11}$  at 400 hertz. It can be shown that comparing  $Z_{12} \pm 180^\circ$  with the unstable load determined from  $GH$  (non-feedback side)  $\pm 180^\circ$  will yield the correct stability information for the non-feedback side. For all of the amplifiers tested,  $Z_{11}$  never caused instabilities while  $Z_{12}$  for the one tuning capacitor case presented the greatest possibility of instability. It is for this reason that the stability predictions and calculations for this study are based only on this single tuning capacitor configuration.

#### D. CURVE COMPARISON

Figure 21 illustrates a composite plot versus frequency of the  $-Z_{12}$  for a typical motor and the  $Z$  unstable for an amplifier. The plot of  $-Z_{12}$  is presented because, as previously explained, in all the cases examined,  $Z_{11}$  never made the amplifier unstable. The loop gain which involved  $Z_{12}$  exhibited tendency for instability in both the one and two tuning capacitor cases, but the former was more severe. The stability criterion mentioned in Figure 21 indicates when the open-loop gain transfer function has no poles in the right half plane. The curve comparison technique is simply a quick method to examine the overlayed motor/amplifier characteristics to perform a simplified Nyquist stability analysis. The value of the loop gain ( $LG$ ) is

$$|LG| = |Z_{12}| / |Z_{\text{unstable}}|$$

because  $|LG| = |GHZ_L|$

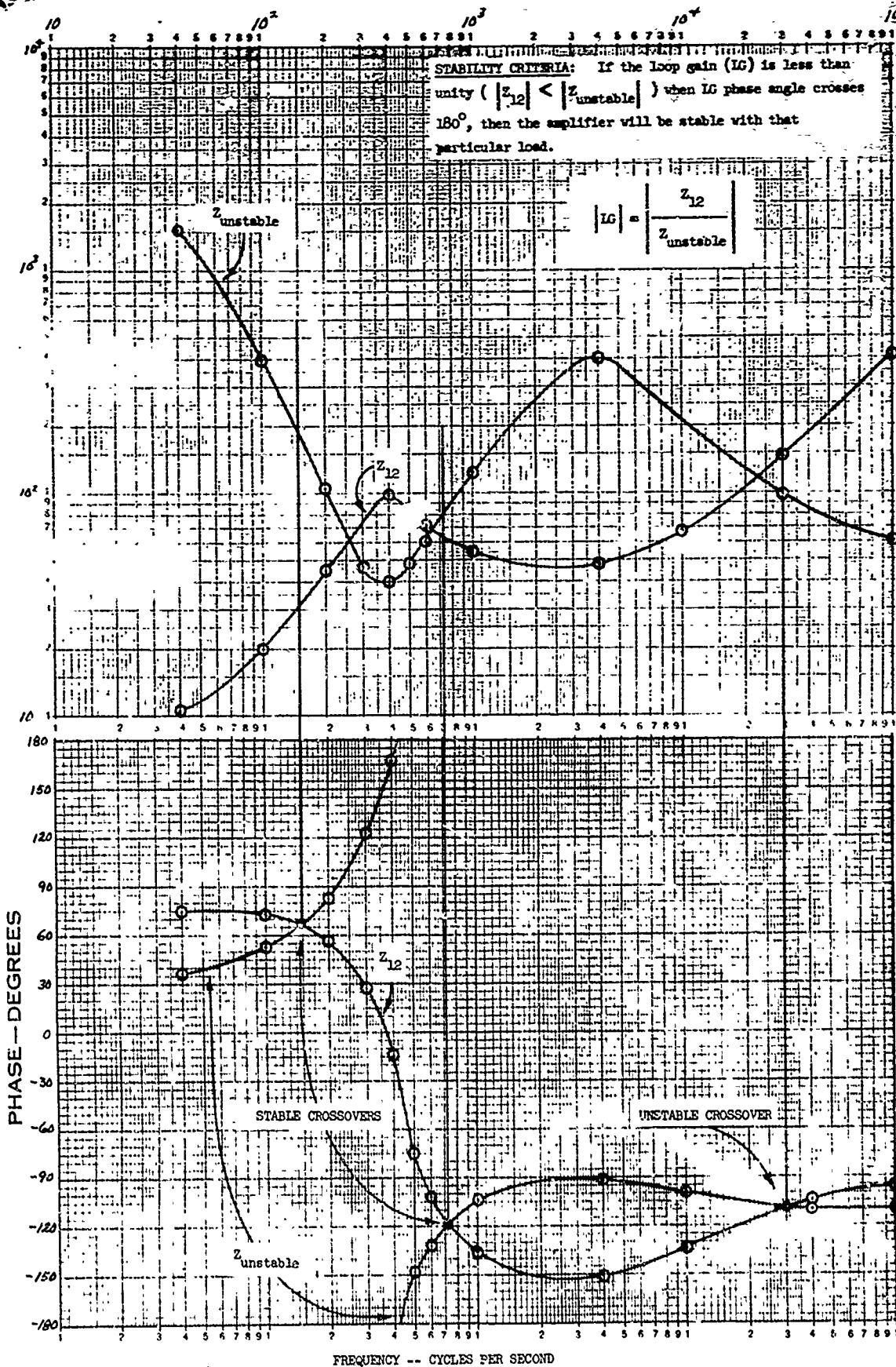
and  $|Z_{\text{unstable}}| = \frac{1.0}{|GH|}$

The  $|LG| = 1$  when the magnitude curves cross, and the  $\angle LG = \pm 180^\circ$  when the phase angle curves cross. The stability criterion is determined from Nyquist stability analysis which indicates right half plane poles if the point  $(-1, 0)$  is encircled by the polar plot of  $LG$ . Further discussion of the stability criteria is presented in Chapter VII.

NOT REPRODUCIBLE

NAFI TR-1331

# FREQUENCY RESPONSE DIAGRAM



NOT REPRODUCIBLE

Figure 21 Comparison of  $Z_{12}$  and  $Z_{unstable}$  Curves to Determine Stability

## VII. STABILITY DETERMINATION TECHNIQUES

### A. DUMMY LOAD DETERMINATION

#### 1. Worst-Case Circuits

As explained previously, the motor equivalent series circuit parameter value limits were represented in a matrix of 16 circuit cases for each motor size (see Figure 8). The circuits in each group were converted into more complex circuits which required missing parameter value determination. The individual circuit in each group that exhibits the most unstable characteristics will represent that size motor as the worst-case stability circuit. In agreement with this, the circuit that presents the greatest opposition to amplifier output power (i.e., causes minimum output power) will be the worst-case power circuit. This worst-case condition was chosen to determine if the amplifiers could deliver an acceptable (minimum) amount of power to the load. Another possible worst-case condition is that load which causes maximum power to be delivered by the amplifier which would indicate whether the output stages could withstand maximum load current. The latter worst-case power condition was not considered in this study. This means that each of these worst-case circuits contain the worst possible parameters combination in their respective sample motor group. Since the other circuits possess better power or stability characteristics, an amplifier that operates satisfactorily with the worst-case circuits will perform better with any other sample motor within that group.

#### 2. Dummy Loads

a. General - With dummy loads that simulate the equivalent circuit in Figure 5 for nominal, worst-case stability, and worst-case power, amplifier parameters such as stability, power output, gain, phase shift, linearity, and temperature range performance can be measured or determined. For proper dummy load simulation at temperatures above or below room temperature, the temperature-sensitive motor parameters in the equivalent circuit must be projected from their normal temperature value to the

motor test temperature. Table VII lists the worst-case dummy load parameters projected to +125°C. This permits amplifier testing at desired temperatures while the loads remain at room temperature. Also, this eliminates the improper load simulation possible with dummy load component value changes due to temperature cycling. Substituting a qualified transformer and low tolerance decade boxes for the parameters in Figure 5 would provide rapid practical motor simulation for several motor sizes with the same dummy load. With this type dummy load based on practical correlated motor specifications, incoming inspection acceptance tests can virtually assure servo amplifier/motor combination compatibility. Another very important point is that the dummy load motor parameter values have to be determined only once.

b. Computer-Aided Solution Technique - Driving-point impedance ( $Z_{11}$ ) and transfer impedance ( $Z_{12}$ ) are the major motor parameters as seen by the amplifier. In fact, these impedance magnitudes and angles must simulate actual motor performance for the amplifier. Worst-case motor load simulation is accomplished by reducing all of the worst-case equivalent circuit parameter values into their usable impedance equivalents ( $Z_{11}$  and  $Z_{12}$ ). The magnitudes and angles are calculated by a computer program. The printout of the card fortran version and the time-sharing basic version of this program are illustrated in Figures 22 and 23. Table VIII defines the variables used in these computer programs. This program solves equations 7-1 and 7-2 for  $Z_{11}$  and  $Z_{12}$ . These equations are developed in NAFI TR-1053.

$$Z_{11} = \frac{1}{4} \left[ \frac{1}{SC_T + \frac{1}{R_{DC} + SL - \frac{S^2 K^2 L^2}{R_R + SL}}} + R_{DC} + SL_{LP} \right] \quad (7-1)$$

$$Z_{12} = -\frac{1}{4} \left[ \frac{1}{SC_T + \frac{1}{R_{DC} + SL - \frac{S^2 K^2 L^2}{R_R + SL}}} - R_{DC} - SL_{LP} \right] \quad (7-2)$$

TABLE VII Worst-Case Dummy Loads  
(PARAMETER VALUES ARE PROJECTED TO  $\pm 125^{\circ}\text{C}$  AMBIENT)

SERIES EQUIVALENT					COMPLEX EQUIVALENT					
TYPE LOAD	CASE NO.	$R_{bc}$ (OHMS)	$R_{ac}$ (OHMS)	$X_{Ls}$ (CHMS)	$RI(R_{bc})$ (OHMS)	$LI$ (mh)	K	L (mh)	$R_k$ (OHMS)	$C_T$ (uf)
WORST	871	168	44.1	220.7	168	2.6	.6	129	148.5	1.43
CASE	1171	69.5	139.4	253.3	69.5	2.6	.8	171.8	309.5	1.65
STABILITY	1571	27.5	57.3	123.5	27.5	2.6	.76	82.5	153.1	3.3
WORST	870	168	44.1	220.7	168	2.6	.6	129	148.5	1.17
CASE	1170	69.5	139.4	253.3	69.5	2.6	.8	171.8	309.5	1.35
POWER	1540	10	55.8	179.8	10	2.6	.7	104.9	156.5	2.7

	F-07-62-22	00
	DIMENSION F(13)	10
C	PROGRAM CONVERTED FROM TIME-SHARING PROGRAM Z12EQU	20
	READ 40,(F(I),I=1,13)	30
	40 FORMAT (13I6)	90
	45 READ 50,N,R1,EL1,EL,R4,CAY,C	100
	50 FORMAT (I6,F6.2,F6.3,F6.4,F6.1,F6.2,E9.2)	110
	IF((N/10)*10-N)60,80	120
	60 PRINT 70,N	130
	70 FORMAT (////24X,9HCASE NO. ,I4//)	140
	GO TO 95	150
	80 PRINT 82	160
	82 FORMAT (1H1,2X,60HSERVO MOTOR DRIVING-POINT (Z11) AND TRANSFER IMPEDANCE (Z12))	163
	85 PRINT 90,N	165
	90 FORMAT (////24X,9HCASE NO. ,I4,//)	170
	95 PRINT 100	180
	100 FORMAT(4X,9HFREQUENCY,4X,8HZ11(MAG),4X,8HZ11(ANG),4X,8HZ12(MAG),4X,190	
	28HZ12(ANG),4X,8HPWR LOAD/)	200
	I = 1	210
	110 W = 2*3.14159265*F(I)	220
	EL4 = (1-CAY)*EL	230
	EL6 = EL4-EL1	240
	EL5 = CAY*EL	250
	EM4 = R4*R4+(W*EL4)**2	260
	E5 = R4/EM4	270
	EYE5 = 1/(W*EL5)+W*EL4/EM4	280
	EM5 = E5*E5+EYE5*EYE5	290
	E3 = E5/EM5	300
	EYE3 = EYE5/EM5+W*EL6	310
	E7 = R1+E3	320
	EYE7 = W*EL1+EYE3	330
	EM7 = E7*E7+EYE7*EYE7	340
	E8 = E7/EM7	350
	EYE8 = -(EYE7/EM7-W*C)	360
	EM8 = E8*E8+EYE8*EYE8	370
	E9 = (R1-(E8/EM8))/4	380
	EYE9 = (EYE8/EM8+W*EL1)/4	390
	Z9 = SQRTF(E9*E9+EYE9*EYE9)	400
	T9 = ATANF(EYE9/E9)*57.296	410
	J = 0	420
	J1 = 1	430
	IF(E9)279,278	450
	278 J = 1	460
	279 IF(EYE9)281,280	470
	280 J1 = -1	480
	281 T9 = T9+J*J1*180	490
	P1 = (R1+E8/EM8)/4	500
	P2 = (W*EL1-EYE8/EM8)/4	510
	P3 = SQRTF(P1*P1+P2*P2)	520
	P4 = ATANF(P2/P1)*57.296	530
	P5 = P3*COSF(P4/57.296)	532
	PRINT 340,F(I),P3,P4,Z9,T9,P5	540
	340 FORMAT (I11,F14.4,4F12.4)	550
	IF (I-13)350,45	560
	350 I = I+1	570
	GO TO 110	580
	END	590

Figure 22 Printout of Program to Calculate Load Impedances  $Z_1$  and  $Z_2$   
(Card FORTRAN Version)

NAFI TR-1331

```

10 REM PROGRAM TO CALCULATE SM DRIVING-POINTS(Z11) AND TRANS-
020 REM FER (Z12) IMPEDANCES. ENTER DATA IN LINES 900-998 IN
030 REM THE FOLLOWING ORDER: INIT. FREQ., RDC, LEAKAGE, L, RZTRP
040 REM RES., K, CAP., NO. OF ADDITIONAL FREQS, ADDITIONAL FREQ
050 REM VALUES. ENTER CASE # IN LINE 800
060 LET I=1
100 READ X,F,P1,L1,L,P4,K,C,N
102 PRINT
104 PRINT "CASE":X
106 PRINT
110 PRINT "FREQUENCY","Z11(MAG)","Z11(ANG)","Z12(MAG)","Z12(ANG)"
112 PRINT
120 LET W=2*3.14159265*F
130 LET L4=(1-K)*L
140 LET L6=L4-L1
150 LET L5=K*L
160 LET M4=P4*R4+(W*L4)^2
170 LET E5=R4/M4
180 LET I5=1/(W*L5)+W*L4/M4
190 LET M5=E5*E5+I5*I5
200 LET E3=E5/M5
210 LET I3=I5/M5+W*L6
220 LET E7=R1+E3
230 LET I7=W*L1+I3
240 LET M7=E7*E7+I7*I7
250 LET E8=E7/M7
260 LET I8=(I7/M7-W*C)*(-1)
270 LET M8=E8*E8+I8*I8
271 LET E9=(R1-E7/M8)/4
272 LET I9=(I8/M8+W*L1)/4
273 LET Z9=SQR(E9*E9+I9*I9)
274 LET T9=ATN(I9/E9)*57.296
275 LET J=0
276 LET J1=1
277 IF E9<0 THEN 279
278 LET J=1
279 IF I9<0 THEN 281
280 LET J1=-1
281 LET T9=T9+.1*J1*180
283 LET P1=(R1+E8/M8)/4
285 LET P2=(W*L1-I8/M8)/4
288 LET P3=SQR(P1*P1+P2*P2)
290 LET P4=ATN(P2/P1)*57.296
330 PRINT F,P3,P4,T9
340 IF I>N THEN 999
350 READ F
360 LET I=I+1
370 GO TO 120
900 DATA 170
900 DATA 1200
902 DATA 64
904 DATA 3E-3
906 DATA .107,217,.73
912 DATA 1.53E-6
914 DATA 2,400,100
999 END

```

Figure 23 Printout of Program to Calculate Load Impedances  $Z_{11}$  and  $Z_{12}$   
(Time-Sharing BASIC Version)

TABLE VIII

DEFINITION OF VARIABLES USED IN THE COMPUTATION OF  
 $Z_{11}$  AND  $Z_{12}$

ITEM NO.	INPUT VARIABLE		DEFINITION
	CARD FORTRAN	TIME SHARING BASIC	
1	CAY	K	The coupling coefficient between the stator & rotor.
2	C	C	Tuning capacitor value.
3	EL1	L1	Leakage inductance.
4	EL	L	Magnetizing inductance.
5	N	X	Case no.
6	R1	R1	$R_{oc}$
7	R4	R4	$R_r$ = Rotor resistance.



c. Worst-Case Stability - The impedance (magnitude and angle) of  $-Z_{12}$  for each different combination of extreme motor parameters (see Figure 8) were compared with the amplifier  $Z_{\text{unstable}}$  (magnitude and angle) at various frequencies. The combination of motor parameters which resulted in the greatest possibility of causing instability was the set of parameters which resulted in the largest absolute value of the angle of  $(Z_{12})$  near 1200 hertz. This most unstable condition occurred with the amplifier at maximum temperature and the motor equivalent circuit projected from the average motor ambient temperature to this maximum temperature. The following conditions were the same for sizes 8, 11, and 15 servomotors:

(1) The matrix case number was 71. Checking this case number in the matrix of possible loads (Figure 8) shows that the equivalent circuit parameter values for the worst-case stability dummy load have definite value trends:  $R_{0c}$ ,  $X_{1s}$ , and  $C_1$  are maximum, and  $R_s$  is minimum.

(2) The operating temperature was maximum. Generally, as the amplifier  $Z_{\text{unstable}}$  magnitude and absolute value of angle  $Z_{\text{unstable}}$  decrease with increasing temperature, the motor  $Z_{12}$  magnitude and absolute value of the angle of  $Z_{12}$  increases with increasing temperature. Thus, the possibility that instability may occur increases. This shows that an amplifier/motor combination operating normally at room temperature can very easily become unstable at increased temperatures.

d. Worst-Case Power - As previously mentioned, the worst-case power equivalent motor circuit as defined in this report causes minimum amplifier output power. The matrix case numbers that fulfilled this requirement contained the maximum real component of driving-point impedance ( $Z_{11}$ ) (i.e., the maximum  $|Z_{11}| \cos \angle Z_{11}$ ). Like the worst-case stability tests, the worst-case (W.C.) power conditions occur at maximum temperature. These worst-case circuit values are also projected to their proper values at the maximum motor operating temperature. The sizes 8 and 11 worst-case power circuits are the same as the sizes 8 and 11 worst-case stability circuits, respectively, with one exception. The tuning capacitor ( $C_1$ )

value is minimum for W.C. power and maximum for W.C. stability. For the size 15 motors, the W.C. power dummy load corresponded to case 40 of the matrix in Figure 8. The equivalent circuit parameters corresponding to this case are:  $R_s$  is a maximum;  $R_{dc}$ ,  $X_{ls}$ , and  $C_T$  are a minimum. Table IX below reviews the worst-case power dummy load parameter conditions.

TABLE IX PARAMETER LIMITS FOR WORST-CASE POWER DUMMY LOADS			
Item	Parameter	Size 8 & 11 Motors	Size 15 Motor
1	Matrix Case No.	70	40
2	Temperature	Max	Max
3	$R_{dc}$	Max	Min
4	$R_s$	Min	Max
5	$X_{ls}$	Max	Min
6	$C_T$	Min	Min

### 3. Load Implementation

Once these worst-case and nominal load parameters are determined, there still remains the problem of implementing the load by actual components for laboratory tests. The most difficult item in the equivalent circuit to simulate is the ideal transformer. The CODED-"T" automatic transformer design computer program was used to obtain a design which would approximate the ideal transformer characteristics. Figure 24 is the computer printout of the performance and construction data for the transformer design which was used for the simulation of all three sizes of motor loads. The resistances in the dummy loads were simulated by selected carbon composition resistors and the inductances by decade inductance boxes. The transformer leakage inductance was used to represent the leakage between halves of the control winding. When calculating the values for the external resistors and inductors,



POWER TRANSFORMER DESIGN READOUT

PART 2- ELECTRICAL PARAMETERS (CODED SERIAL NUMBER= 710461)

	1	2	3	4	5	6	7	8	9
A. WINDING RATINGS									
WINDING NUMBER	PRIM	SEC							
WINDING DESIGNATION	72.4	87.0							
POWER (VOLT-AMPS)									
VOLTAGE RATINGS									
FULL LOAD VOLTAGE	115.0	111.7							
NO LOAD VOLTAGE	115.0	120.6							
TAP VOLTAGE	57.5	0.9							
VOLTAGE REGULATION (PCT)		6.2							
TOLERANCE REQUESTED (PCT)		5.0							
CURRENT RATINGS (MILLIAMPS)									
RMS CURRENT	667.0	600.0							
D.C. CURRENT	10.0	0.0							
IMPEDANCE (OHMS)									
WINDING RESISTANCE	4.6	9.6							
RESISTIVE LOSS		18.1							
CAP. REACTANCE TO CORE	2005.3	309.19							
PARAMETERS OF SECONDARIES REFERRED TO	HE	PRIMARY							
PHASE SHIFT (DEGREES)		4.0							
LEAKAGE INDUCT (MILLIHMS)		4.3							
INDUCTIVE REACTANCE (OHMS)		19.9							
INTERVINDING CAP. (PMK)		1907.2							
CAP. REACTANCE (KILOHMS)		153.2							
SIZE (MAXIMUM) DOES NOT INCLUDE									
VOLUME	55.370	CUBIC INCHES							
OVERALL DIMENSIONS									
HEIGHT (IF DIRECTION)	3.500	INCHES							
WIDTH (IF DIRECTION)	3.500	INCHES							
LENGTH (IF DIRECTION)	4.920	INCHES							
GENERAL RATINGS									
EFFICIENCY	92.5	PERCENT							
FLUX DENSITY	16545	GAUSS							
MAXIMUM FREQUENCY	4000.0	CPS							
MINIMUM FREQUENCY	40.0	CPS							
RESONANT FREQUENCY	391.73	DEGREES							
AMBIENT TEMPERATURE	100	DEGREES							
TEMPERATURE RISE	10	DEGREES							
TEMPERATURE CLASS									
OPERATING LIFE	200000	HOURS							
D. GENERAL PARAMETERS									
CORE LOSS	0.0	WATTS							
COPPER LOSS	3.4	WATTS							
EXCITATION LOSS	2.9	VOLT-AMPS							
MAGNETIZING VARS									
CORE LOSS CURRENT (INCH)							0.009	AMPS	
MAGNETIZING CURRENT (MAX)							0.124	AMPS	
IRON SHUNT RESISTANCE							OVER 9999	OHMS	
IRON SHUNT REACTANCE							OVER 4883	OHMS	

Figure 24 Continued

the effect of the transformer internal parameters (e.g., secondary leakage,  $R_{sc}$ , and turns ratio) should be compensated for when possible, for more accurate simulation.

The magnetizing impedance of the transformer is high compared to the secondary load, so the leakage inductances, DC resistances, and turns ratio are the only parameters of significance. The experimentally determined transformer parameters are:

DC resistance (pri.)	= 4.5 ohms
DC resistance (sec.)	= 9.3 ohms
Leakage inductance (pri.)	= 2.6 mh
Leakage inductance (sec.)	= 2.6 mh
Turns ratio ( $N_p/N_s$ )	= 0.907:1

#### 4. Load Comparisons (Practical, Ideal, and Experimental)

Once the parameter values were calculated for the loads using practical components, an analysis of  $Z_{12}$  versus frequency using the CODED computer circuit analysis program for the practical loads (Figure 26) was performed and compared with the desired frequency responses of the ideal loads (see Figure 5). These loads were constructed in the laboratory, and the  $Z_{12}$  responses were determined experimentally. Figure 25<sub>2</sub> illustrates the comparisons between the  $Z_{12}$  responses for the ideal (Figure 5), practical (Figure 26), and experimental (Figure 27) worst-case stability loads for size 8 motors. It is thought that the reason for the disagreement in the experimental curve at high frequencies is caused by inaccurate prediction of the transformer distributed capacitances which have a significant effect.

Also, on the same drawing the  $Z_{12}$  of the practical equivalent series dummy load (Figure 28a) is plotted to illustrate the differences. It should be noted that the equivalent series dummy load differs significantly from the others at frequencies below the carrier frequency. The importance of this will be discussed later. Figure 25b also illustrates

NAFI TR-1331

these differences and the effect of changes in K for complex loads.  
The  $Z_{12}$  curves in Figure 25b are for ideal dummy loads for the size 8 motor.

# FREQUENCY RESPONSE DIAGRAM

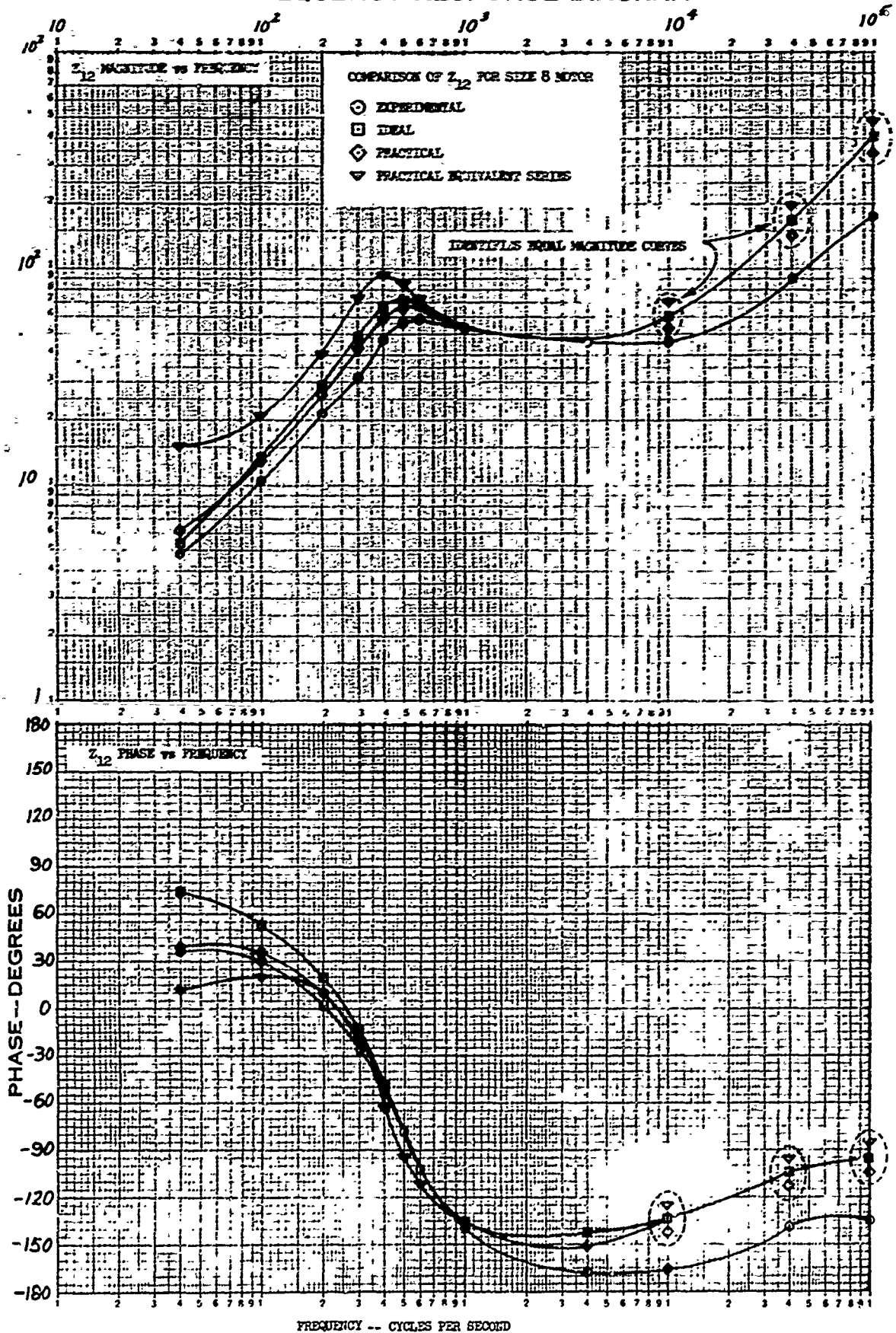
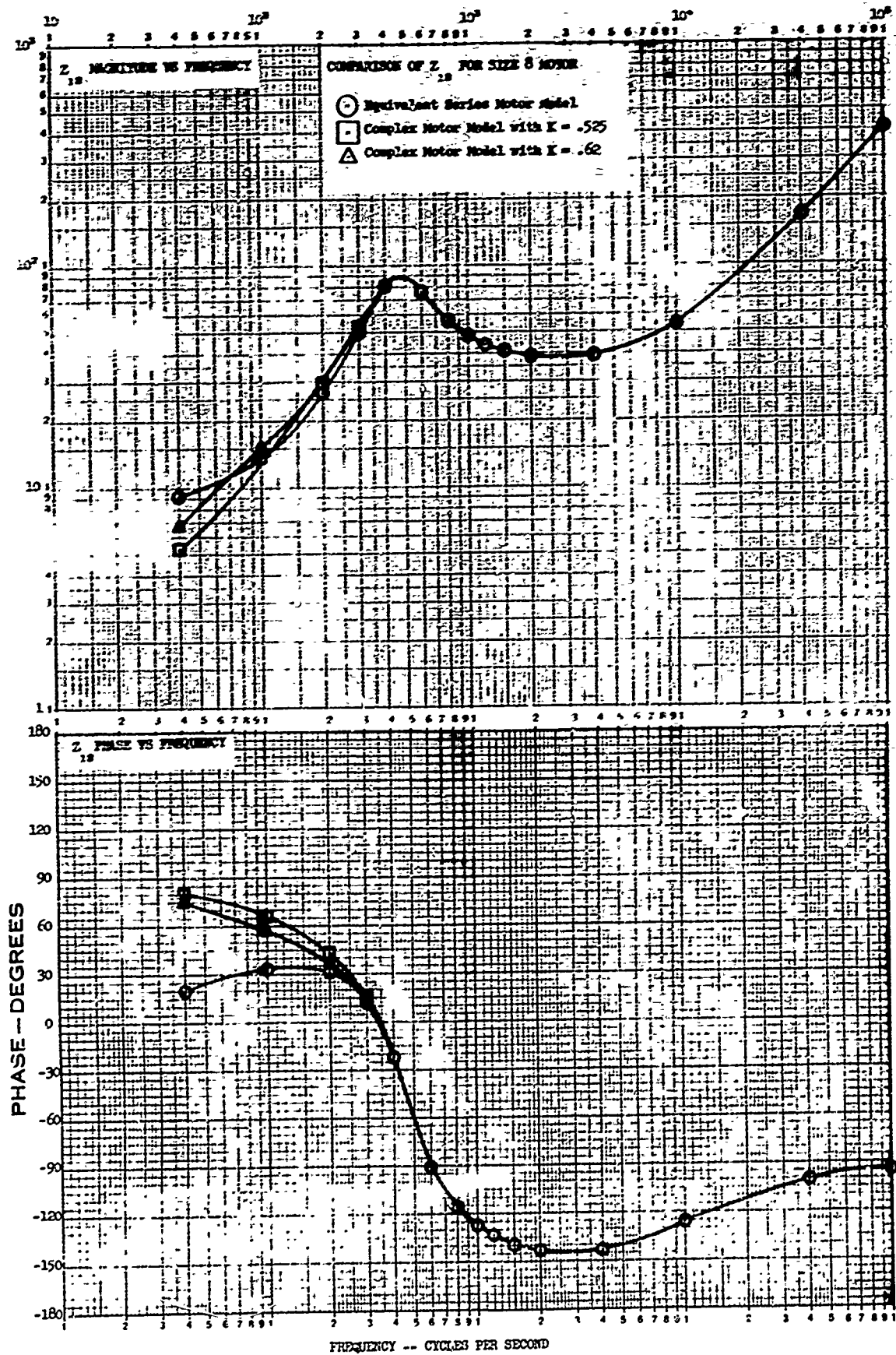


Figure 25a Comparison of  $Z_{12}$  Responses

# FREQUENCY RESPONSE DIAGRAM


Figure 25b Comparison of  $Z_{1s}$  Responses



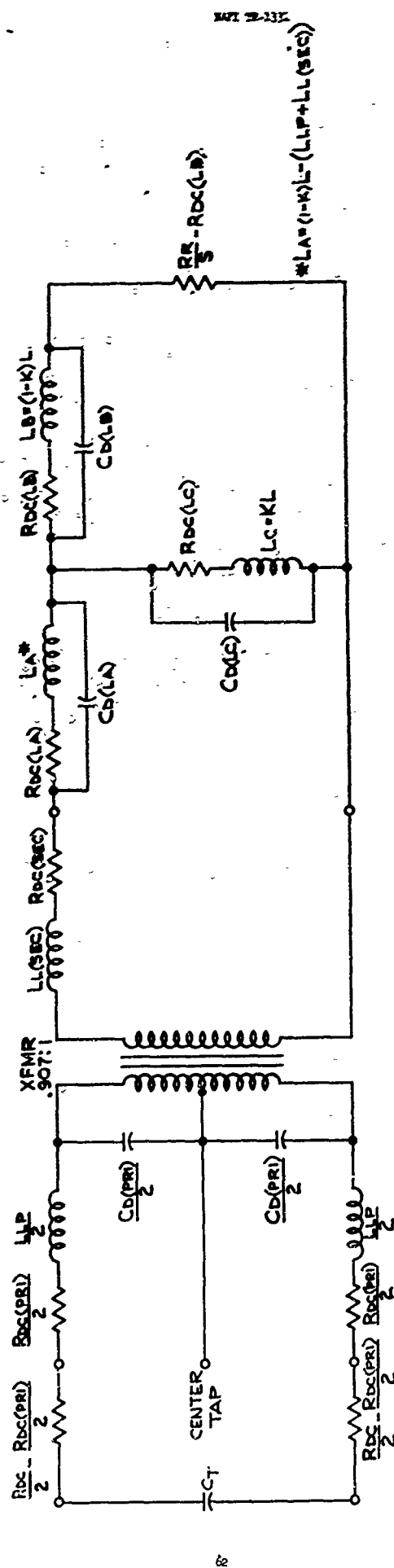


FIG. 26 PRACTICAL DUMMY LOAD FOR THE COMPLEX EQUIVALENT CIRCUIT MOTOR MODEL

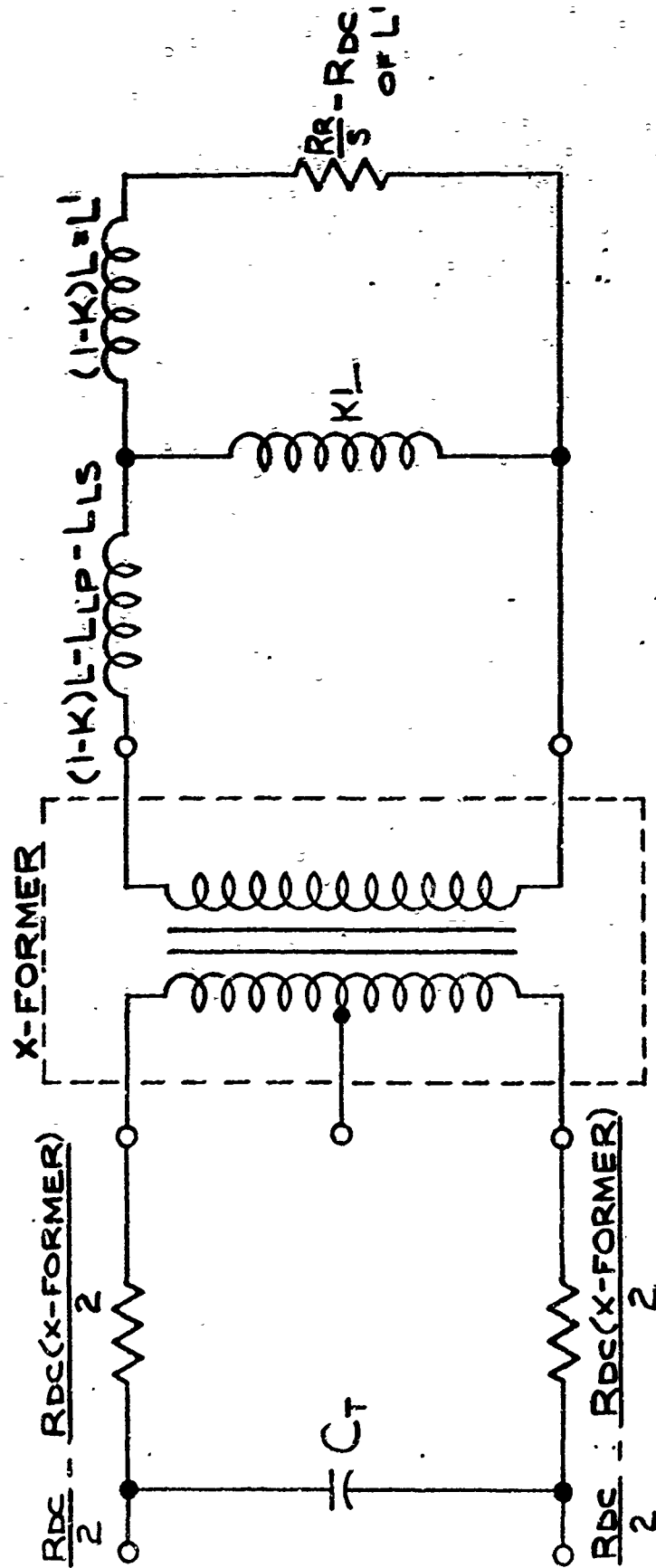


FIG. 27 EXPERIMENTAL DUMMY LOAD FOR THE  
EQUIVALENT CIRCUIT MOTOR MODEL

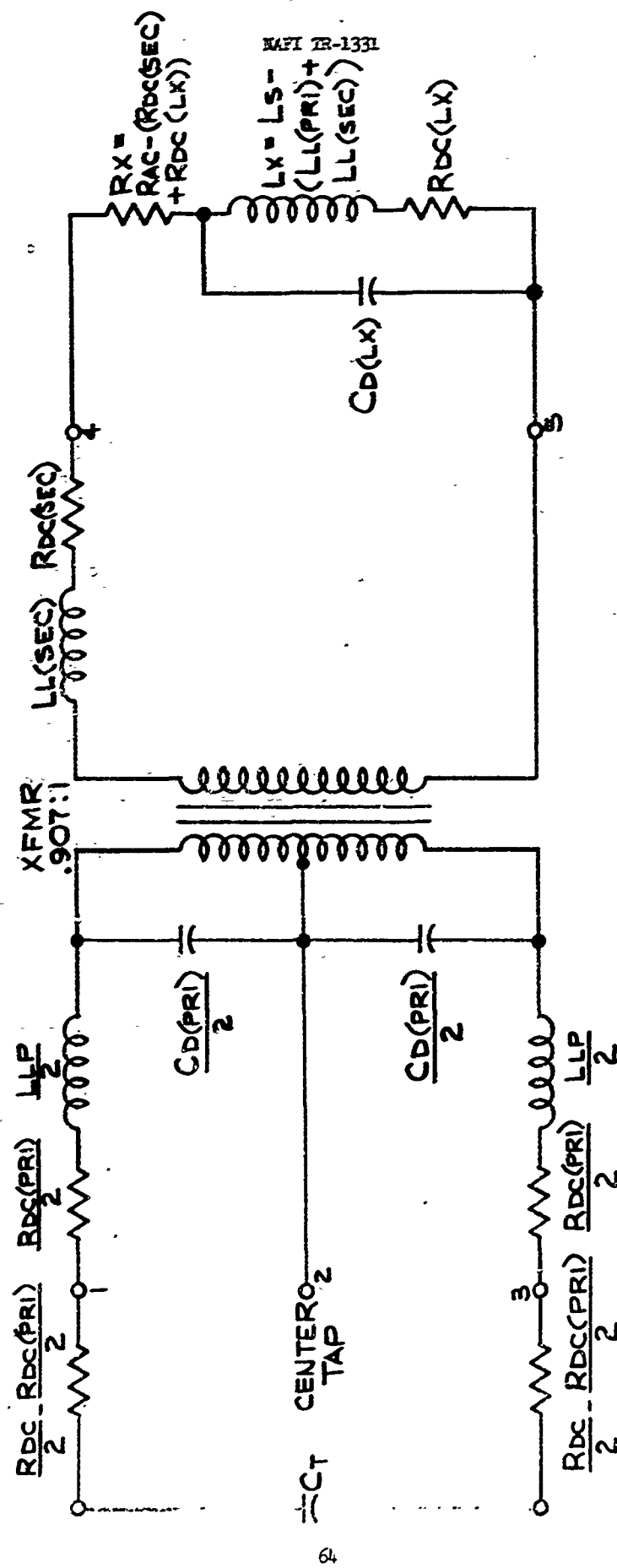


FIG. 28a. PRACTICAL EQUIVALENT SERIES DUMMY LOAD

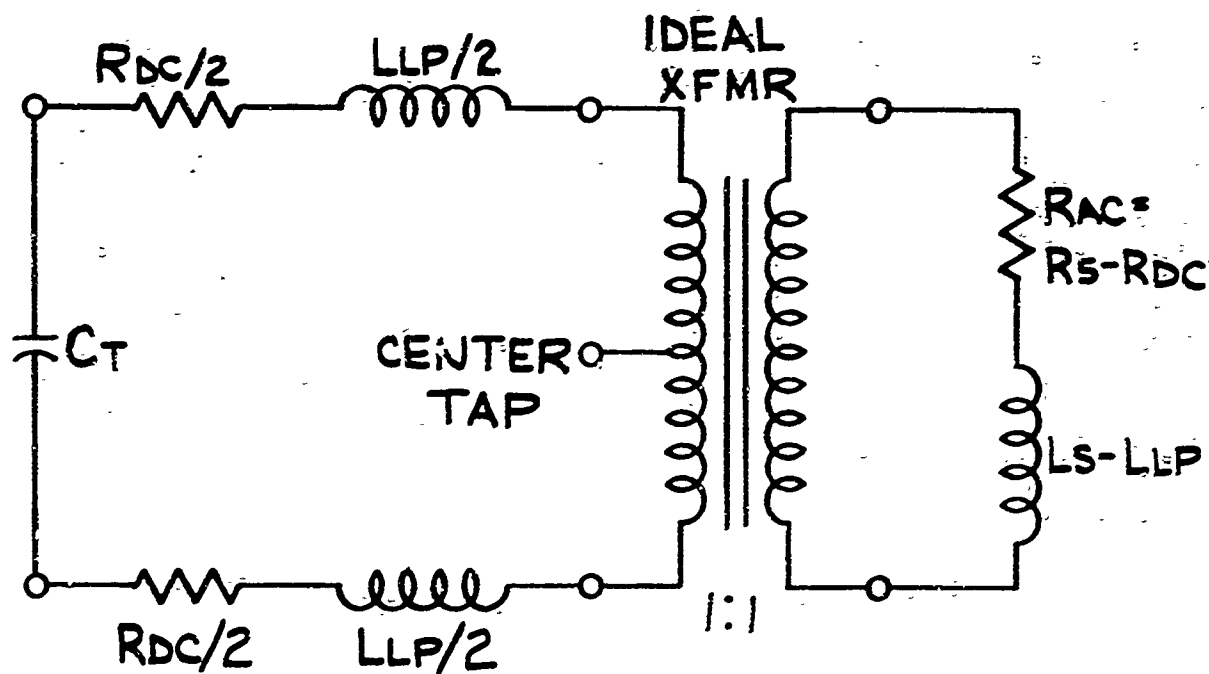


FIG. 28b. IDEAL EQUIVALENT SERIES DUMMY LOAD

## B. TESTING PROCEDURE (AMPLIFIER WITH WORST-CASE DUMMY LOAD)

All of the amplifiers which have an output power rating of approximately 3.5 watts were tested with the size 8 and size 11 servo-motor dummy loads while all of the high-powered amplifiers were tested with only the size 15 dummy load. Since the worst-case (as far as stability is concerned) is when the amplifier temperature is highest (resulting in highest amplifier gain), the amplifiers were all placed in an oven at their maximum rated case temperatures. To avoid having to implement a dummy load which duplicated the motor temperature dependence characteristics, the dummy load was kept outside the oven. All temperature dependent parameter values of the equivalent circuit were projected up in temperature to the maximum. This maximum motor temperature was determined by adding the temperature rise caused by the fixed phase winding being energized to the maximum ambient temperature (+125°C) for the motors.

With the amplifier and dummy load at the proper temperatures, a transfer characteristic plot (see Figures 30, 31, and 32) was made utilizing a demodulator test set designed and built at NAFI and a X-Y recorder. A great deal of information can be obtained from these plots such as low frequency stability, gain, gain linearity, phase shift, saturated output voltage, and cross-over distortion. The function of the demodulator test set is to provide an amplitude modulated input 400 Hz signal to the amplifier and to demodulate both the input signal and the amplifier output signal. The test set provides DC output signals for the X-Y recorder which are proportional to both the in-phase and quadrature components of the demodulated signals.

## C. COMPARISON OF PLOTS OF $Z$ (unstable) AND $Z_{12}$ FOR WORST-CASE STABILITY DUMMY LOAD

To understand how stability information may be derived from a comparison of the  $Z$  (unstable) curve and the  $Z_{12}$  curve for the worst-case

stability dummy load, the definition of  $Z$  (unstable) must be recalled. The total amplifier feedback loop gain is defined as  $G(S)H(S)Z_1(S)$  where  $Z_1(S)$  is the complex load on the amplifier, and  $G(S)H(S)$  is independent of the load. For a given frequency, a value of the  $GH$  product may be determined experimentally, and a value of  $Z_1$  can be calculated from the characteristic equation:  $GHZ_1 + 1 = 0$ . This value of  $Z_1$  is that which causes borderline instability and is called  $Z$  (unstable).

Information similar to that obtained from Nyquist stability plots can be obtained from the comparison of these curves. The following equations indicate that the loop gain magnitude at any given frequency is  $|Z_1|/|Z \text{ (unstable)}|$ .

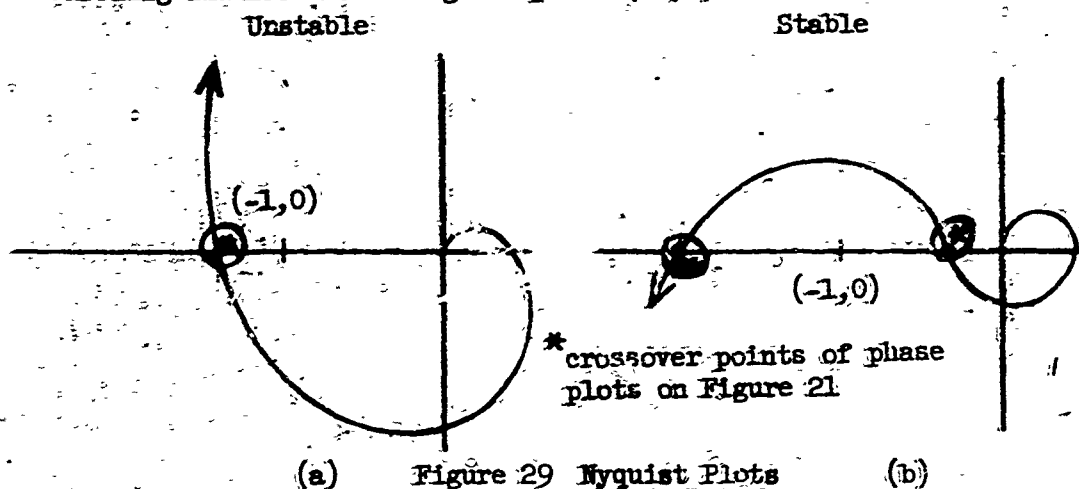
$$|Z \text{ (unstable)}| = \frac{|-1.0|}{|GH|} \quad (7-3)$$

$$|\text{loop gain}| = GHZ_1 \quad (7-4)$$

$$\therefore |\text{loop gain}| = \frac{|Z_1|}{|Z \text{ (unstable)}|} \quad (7-5)$$

Also, the phase angle of the loop gain can be shown to be plus or minus  $180^\circ$  when the  $Z_{12}$  curve crosses  $Z$  (unstable). Therefore, a polar plot of the loop gain can be considered to encircle the point  $(-1, 0)$ , which indicates instability on a Nyquist plot, when the loop gain magnitude is greater than one ( $|Z_{12}| > |Z \text{ (unstable)}|$ ) at a frequency when the loop gain phase angle is plus or minus  $180^\circ$  (at a crossover of the phase curves). Figure 21 illustrates two stable crossovers and one unstable crossover. One cannot blindly assume that meeting the above criteria for encircling the point  $(-1, 0)$  will ensure instability. The actual Nyquist plot (a polar plot of the loop gain) should be sketched from the  $Z_{12}$ ,  $Z$  (unstable), and  $GH$  curves or values. As indicated above, the loop gain magnitude and the points where the loop gain angle equals  $\pm 180^\circ$  can be easily extracted from the comparison of  $Z_{12}$  and  $Z$  (unstable) curves. The loop gain phase angle for any given frequency would be the sum of the phase angles of  $GH$  and  $Z_{12}$ . This sketch of the Nyquist plot should be made at least once for each new amplifier configuration to ensure whether the curve will encircle the point  $(-1, 0)$  in the proper direction or not. For example, the polar plots in Figure 29 (a) and (b) of loop gain pro-

gressing in the direction of increasing frequency, are, respectively, encircling and not encircling the point  $(-1,0)$ .



It was noted when comparing these curves that instabilities never occurred for frequencies below 400 hertz. It should also be noted from the curves in Figure 25 that the equivalent series dummy load (Figure 28)  $Z_{12}$  curve closely matches the more complex dummy load (Figure 26)  $Z_{12}$  curve for frequencies above 400 hertz. Had these facts been known before the testing for this study, the worst-case stability dummy load utilized could have been the simpler equivalent series model (Figure 28). However, to ensure that the dummy load is worst-case for all the frequencies of probable instability, the more complex dummy load (Figure 26) is recommended and was utilized. The simpler equivalent series dummy is, however, fully adequate for nominal and worst-case power dummy load tests on amplifiers, where the 400 hertz value of the load impedance is of primary importance. The more complicated dummy load was utilized for the worst-case power testing because the parameters for this load differed from the worst-case stability load by only the capacitor value for the sizes 8 and 11 motors. The amplifiers were not tested with nominal dummy loads.

#### D. COMPARISON OF THE RESULTS OF THE TWO STABILITY DETERMINATION TECHNIQUES

Table X lists the servo amplifiers that were tested. Table XI

NAFI TR-1331

TABLE X: Servo Amplifiers Tested

IDENTIFICATION CODE	MANUFACTURER	MODEL NO.	SERIAL NO.	TYPICAL LOAD MOTOR SIZE
A	BECKMAN INSTR. INC.	961	19	8 6x 11
B	"	962	21	"
C	BULOVA ELEC. DIV.	261	664440	"
D	"	261	664457	"
E	CLIFTON PRECISION PRODUCTS CO., INC.	41100000	2860	"
F	"	41100000	4486	"
G	CONTROL TECHNOLOGY CO., INC.	200HS	1074	"
H	"	200HS	1075	"
I	"	930	162	"
J	"	930	163	"
K	KEARFOOT DIVISION	0703105009	100	"
L	"	0703105009	101	"
M	"	0703148006	105	"
N	"	0703148006	126	"
O	"	0703516001	1329	15
P	MAGNETICO, INC.	T-256	8	15
Q	"	T4-3A	2016	8 6x 11
R	"	T4-3A	2312	"
S	WESTON INSTR. INC.	U210914-5-25-1-2	20096	"
T	"	U210914-5-25-1-2	20097	"
U	"	U207683-3-40-1-2	20188	15

NAFI TR-1331



NAFI TR-1331

summarizes the stability and power output information obtained from the transfer function characteristics for each amplifier. To evaluate the accuracy of stability predictions using worst-case dummy load testing, the stability prediction information from the frequency responses and from the transfer function plots utilizing dummy loads are summarized and compared in Table XII. Out of a possible total of 38 correlations (matching stability predictions), there were 30 (79% of the total) correlations and 5 (13% of the total) borderline situations. There were only 3 (8% of the total) disagreements in the stability predictions. The reasons for the disagreements were not determined, but only two different amplifiers are involved. The Nyquist plots of these amplifiers were made, but the stability predictions did not change.

It is felt that there is sufficient correlation between the two stability testing methods to allow confidence in the stability predictions utilizing worst-case stability dummy loads. However, if test equipment similar to the demodulator test set is used to determine stability, an oscilloscope should also be used to monitor the amplifier output voltage to detect low level oscillations at frequencies above 400 hertz. These high frequency oscillations would be filtered out by the demodulator if they did not affect the amplitude of the carrier signal significantly.

TABLE XI Transfer Function Plot Characteristics

IDENTIFICATION CODE	LOAD SIZE	WORST CASE STABILITY			WORST CASE POWER		POWER OUT (IN PHASE)		
		STABILITY	DUMMY LOAD	GAIN LINEARITY	DUMMY LOAD PHASE SHIFT	SATURATED			
								condi- tion	max. linear ampl.
A	8	LLO	SLNL	16.5V	+7.55°	+7.67°	2.1W		
B	11	LLO	L	22V	+7.85°	+25.5°	2.5W		
	8	LLO	L	24V	+10.1°	+33.65°	1.8W		
C	11	S	L	25.5V	+9.22°	+35.2°	2.2W		
	8	LLO	L	17V	-17.2°	-24.2°	2.0W		
D	11	LLO	L	25.5V	-10.3°	-30.4°	2.8W		
	8	LLO	L	16.5V	-4.21°	-22.2°	2.3W		
E	11	LLO	L	27.5V	-3.34°	-23.2°	3.0W		
	8	S	L	22.5V	-7.66°	-19.5°	2.4W		
F	11	S	L	32V	-7.4°	-18.05°	3.3W		
	8	S	CD/L	12V	+7.0°	-7.6°	1.7W		
G	11	S	CD/L	13.5	+3.24°	-11.32°	1.0W		
	8	S	L	21V	-14.04°	-39.9°	1.4W		
H	11	S	L	32V	-6.45°	-36.86°	2.2W		
	8	S	L	22V	-24.8°	-44.0°	1.3W		
I	11	S	L	33V	-6.3°	-46.25°	1.6W		
	8	S	SLNL	25V	-34.8°	-19.4°	2.4W		
J	11	LLO	L	27.5	-30.0°	-19.25°	3.3W		
	8	HLO	SEN/L	0	PNA-HLO	-23.0°	2.5W		
K	11	HLO	SEN/L	0	PNA-HLO	-18.9°	3.3W		
	8	HLO	SEN/L	3V	+13.15°	+18.6°	2.3W		
L	11	LLO	L	29V	+2.57°	+18.05°	3.1W		
	8	HLO	SEN/L	6V	+16.1°	+18.2°	2.4W		
M	11	LLO	L	30	+3.11°	+18.1°	3.1W		
	8	S	L	22.5V	-1.72°	+0.94°	2.7W		
N	11	LLO	SLNL	12V	+3.1°	+1.84°	3.6W		
	8	LLO	SLNL	8V	-1.85°	+6.78°	2.6W		
	11	LLO	SLNL	6V	+4.0°	+7.83°	3.6W		

**TABLE XII (Continued)**

IDENTIFICATION CODE	LOAD SIZE	WORST CASE STABILITY		WORST CASE POWER		POWER OUT (IN PHASE)		
		STABILITY	DUMMY LOAD	DUMMY LOAD	SATURATED			
							GAIN LINEARITY	PHASE SHIFT
		max. linear ampl.						
O	15	CNA	SEN	5V	CNA	+24.7°	2.2W	
P	15	HLO	L	17.5V	PNA-HLO	-22.1°	1.2W	
Q	8	LLO	L	22.6V	+2.94°	-41.1°	1.3W	
R	11	S	L	21V	-13.9°	-40.7°	1.3W	
	8	S	L	27V	-8.9°	-41.7°	1.6W	
S	11	LLO	L	15.5V	-8.42°	+10.46°	2.4W	
	8	S	SINL	21.5V	-13.1°	+11.0°	3.2W	
T	11	S	SINL	21.5V	-3.2°	+22.55°	2.1W	
	8	S	SEN	5V	PNA-HLO	+19.6°	2.9W	
U	11	LLO	L	21.5V	+8.4°	20.4°	4.2W	
	15	LLO	SEN	6V	PNA-LLO			
ABBREVIATION CODE		MEANING						
S	Stable							
LLO	Low level oscillations							
HLO	High level oscillations							
L	Linear							
SINL	Slightly nonlinear							
SEN	Severely nonlinear							
CD	Crossover distortion							
PNA	Phase not available - reason							
CNA	Curves not available							

TABLE XII Correlation of Stability Tests

IDENTIFICATION OF AMPLIFIER	MOTOR* SIZE	STABILITY FROM* FREQ. RESPONSE	STABILITY FROM* TRANSFER PCT. PLOT	CORRE-** LATION* CODE
A	8	U	B	B
B	11	S	B	B
	8E	B	S	B
	8I	U	NA	NA
C	11	S	S	+
	8	S	S	+
D	11	S	S	B
	8E	B	S	NA
	8I	U	NA	+
E	11	S	S	+
	8	S	S	+
F	11	S	S	+
	8	S	S	+
G	11	S	S	+
	8	S	S	+
H	11	S	S	+
	8	S	S	+
I	11	S	S	+
	8	S	S	+
J	11	S	U	-
	8	S	U	-
K	8	U	U	+
	11E	B	E	+
	11I	S	NA	NA
L	8	U	U	+
	11E	B	B	+
	11I	B	NA	NA
M	8	S	S	+
	11	S	S	+
N	8	S	S	+
	11	S	S	+
O	15	curves not available	curves not available	NA
P	15	S	U	-
Q	8	S	S	+
	11	S	S	+
R	8	S	S	+
	11	S	S	+
S	8	S	S	+
	11E	S	S	+
	11I	B	NA	NA
T	8	S	S	+
	11	S	S	+
U	15E	B	U	E
	15I	B	NA	NA

TABLE XII (Continued)

\* The letter I indicates ideal load, and the letter E indicates experimental load used in lab tests.

\*\* B - Borderline  
S - Stable  
U - Unstable  
NA - Not applicable

\*\*\* (+) - Plots agree  
(-) - Plots disagree  
B - Borderline  
NA - Not applicable

# VIII. EVALUATION OF SERVO AMPLIFIER PERFORMANCE

## A. CRITERIA FOR EVALUATION OF SERVO AMPLIFIER/SERVOMOTOR COMBINATIONS

### 1. Stability Evaluations Using Motor and Amplifier Frequency Characteristics

The exact criteria for stability prediction using the frequency characteristics comparison was presented in section VII.C. Some small errors exist in the values of the curves due to measurement inaccuracies and computations. The tests were performed on, at most, a sample size of two for any given amplifier model number. Table X lists the amplifiers which were tested. Therefore, the spread of frequency characteristics for a larger sample size would be significantly greater.

All that was done in this situation was to list whether or not the amplifier/load combinations operated solidly in the stable or unstable regions. Combinations which came "close" to being stable or unstable were categorized "borderline". The definition of "close" is somewhat arbitrary, but all combinations were evaluated using the same definition. A combination is considered borderline if (1) at a crossover of the angles of  $Z_{12}$  and  $Z$  (unstable) (loop gain angle =  $180^\circ$ ), the loop gain magnitude ( $|Z_{12}|/|Z \text{ (unstable)}|$ ) is in the range of 0.8 to 1.25 or (2) when the loop gain magnitude is 1.0, the loop gain phase angle is within  $20^\circ$  of  $\pm 180^\circ$ .

### 2. Stability Evaluation Using Transfer Function Characteristics

As indicated previously, only the instabilities which cause major perturbations in the amplitude of the amplifier output will be detected on the output of the demodulator test set. Figure 30 illustrates a transfer function plot of a combination which did not show signs of oscillations while Figures 31 and 32 present X-Y plots which illustrate slight and severe oscillations, respectively.

Higher frequency (greater than 400 hertz) instabilities which cause only very small changes in carrier signal amplitude can be detected by using an oscilloscope to monitor the output voltage waveforms. Since

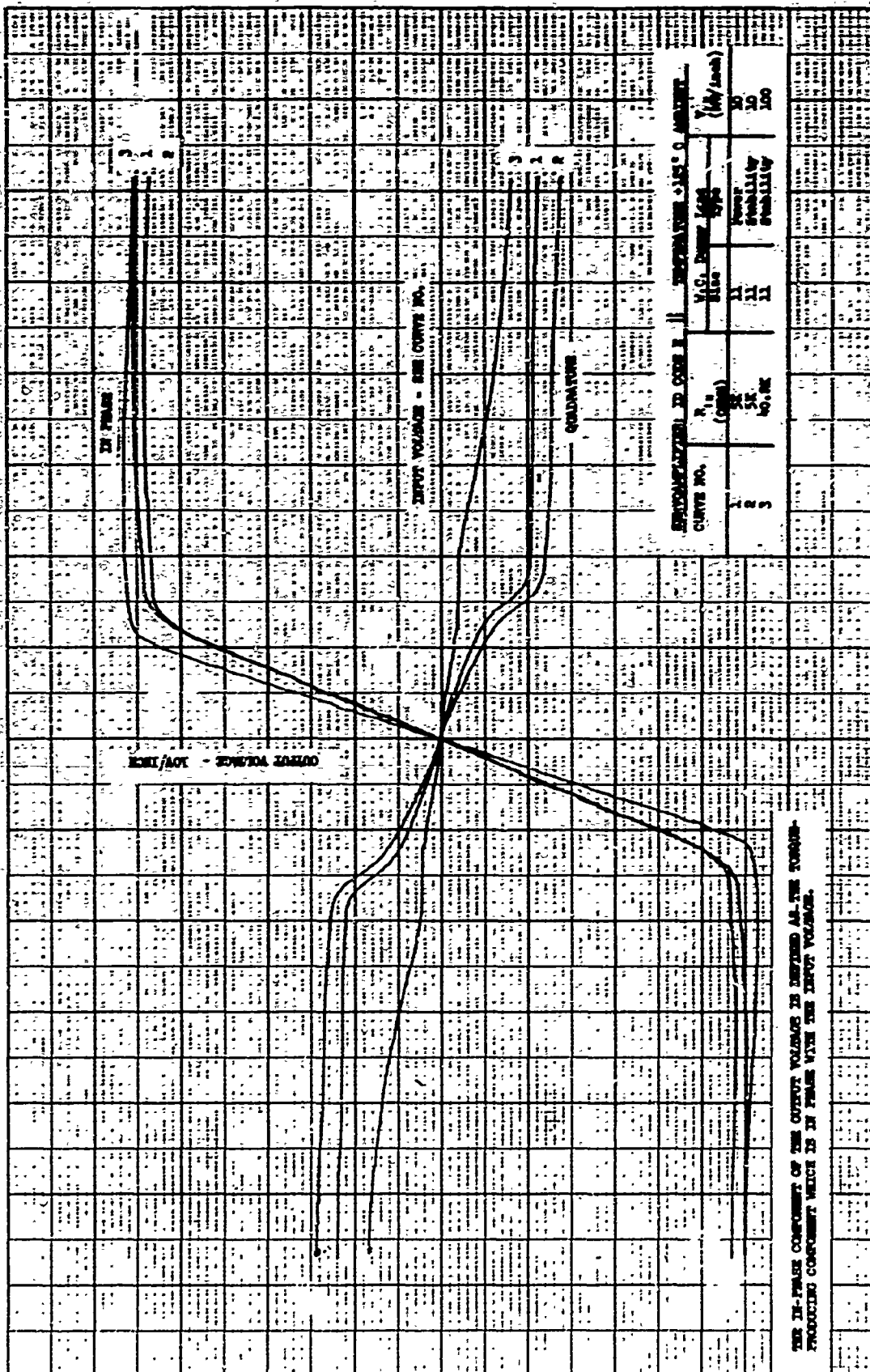


Figure 30 (Continued) 1-1-101

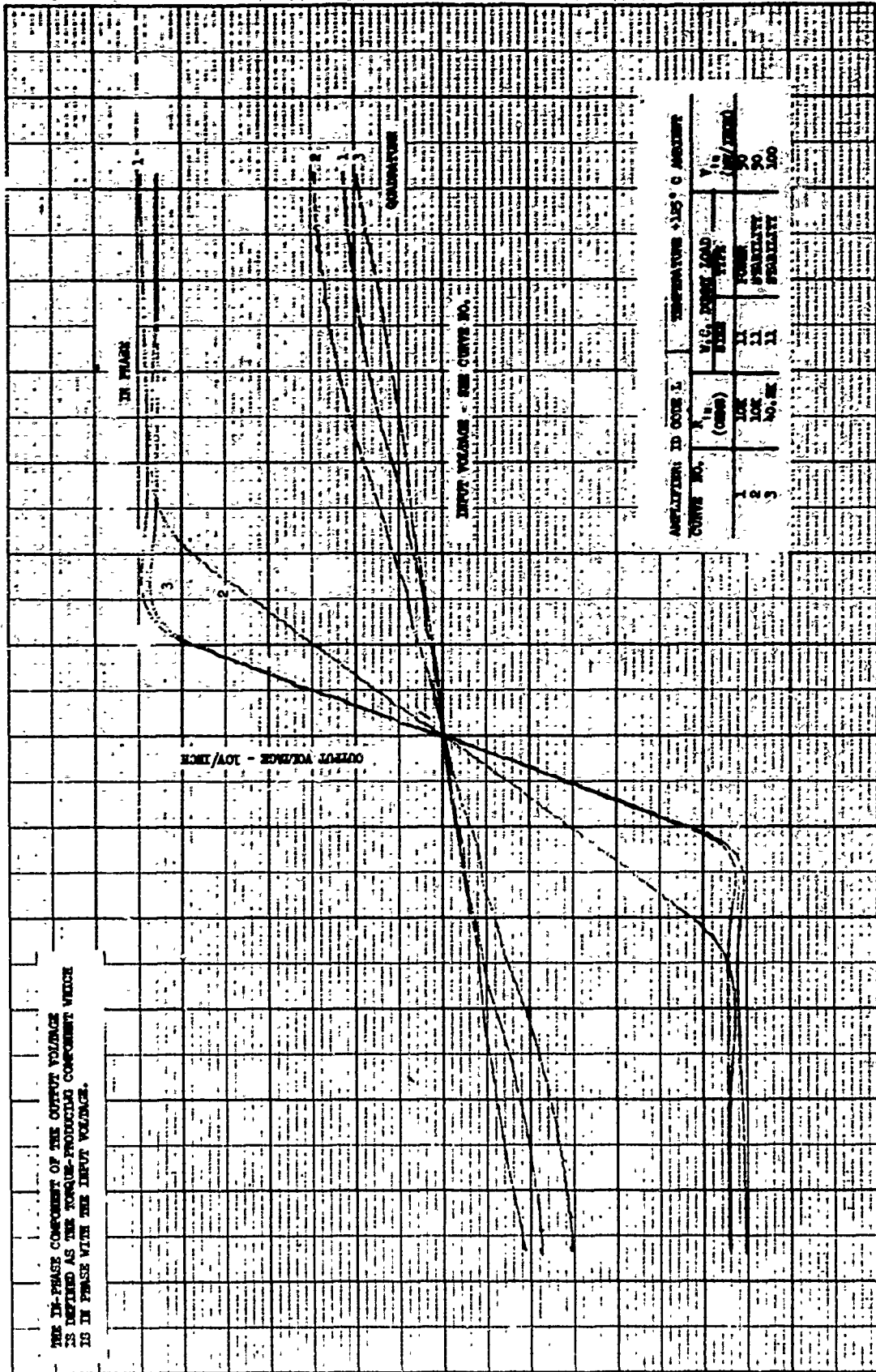


Figure 31. Low Level Oscillating II Plot



NOT REPRODUCIBLE

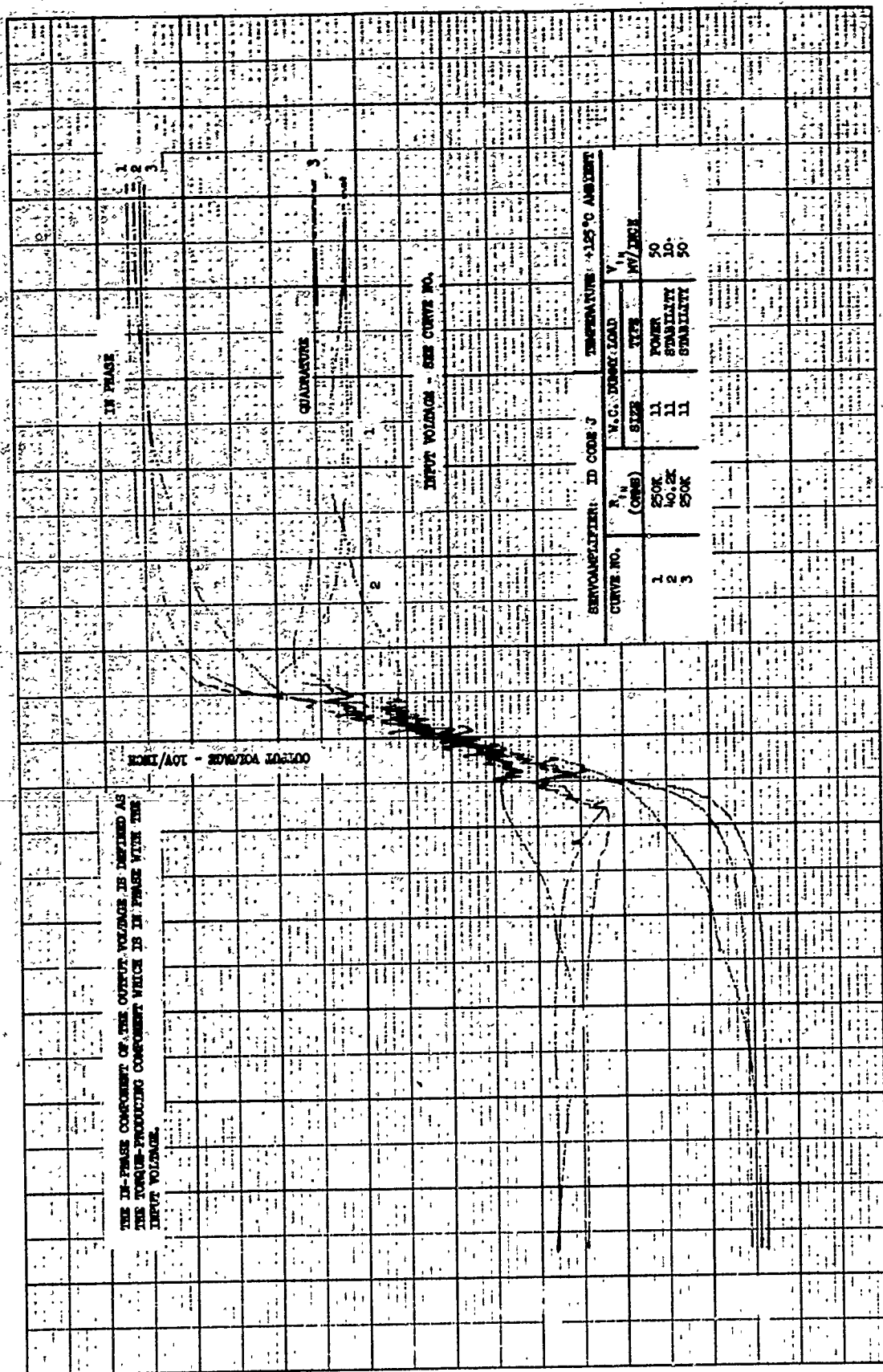


Figure 32 High Level Oscillating XY Plot

these lower amplitude oscillations did not disrupt the gain through the amplifier/load combination, these combinations were not considered important, and the outputs were not monitored with a scope.

### 3. Amplifier Power Output Evaluation

As mentioned previously, the worst-case power dummy load was selected to cause the minimum power output from the amplifiers. The amplifier power output was calculated from the real part of the dummy load impedance (at 400 hertz) and the in-phase component of the output voltage in the saturation region of the transfer characteristics plot. These test results represent the minimum amount of useful power (that which produces torque in the motor) which the amplifier will supply.

### B. SUMMARY OF TEST RESULTS

Table XI summarizes the data taken from the transfer plots for each amplifier. Included in this table are stability and gain linearity information for the worst-case power dummy loads on the amplifiers.

Stability prediction information using both the frequency response comparison method and the transfer function characteristics is presented in Table XII along with the correlation between the two different prediction methods. Since the experimental dummy load frequency characteristics did not agree with those of the ideal dummy load at high frequencies, there occasionally appears a different stability prediction for the ideal and for the experimental load. Only the predictions from the experimental loads were used to correlate with the transfer plot stability predictions.

### C. SUMMARY OF SERVO AMPLIFIER PERFORMANCE

The servo amplifier performance data is presented in Tables XI and XII. It would be more beneficial to present this data and let the reader draw his own conclusions rather than make arbitrary divisions between acceptable and unacceptable performance. However, Table XIII does make predictions of the stability of amplifiers which were tested when connected to any motor with specifications which fall in the ranges given in the recommendations (section II). It should be emphasized that these predictions are based on a very small sample size.

TABLE XIII Summary Of Amplifier Stability

IDENTIFICATION OF AMPLIFIER	MOTOR SIZE	STABILITY PERFORMANCE
A	8	B
B	11	B
C	8	B
D	11	S
E	8	S
F	11	S
G	8	B
H	11	S
I	8	S
J	11	S
K	8	S
L	11	S
M	8	S
N	11	S
O	8	S
P	11	NA
Q	15	D
R	8	S
S	11	S
T	8	S
U	11	B
	15	B
S - Stable B - Borderline Stability NA - Not Available U - Unstable D - Disagreement in Predictions (Amplifier Oscillates)		